# Spreading Processes over Adaptive Networks

Tian Gan

# Spreading Processes over Adaptive Networks

by

## Tian Gan

to obtain the degree of Master of Science
at the Delft University of Technology,
to be defended publicly on Friday November 19, 2021 at 14:00 PM.

Student number:     5028531
Project duration:    January, 2021 – November, 2021
Thesis committee:   Prof. dr. ir. Piet Van Mieghem,     TU Delft, supervisor
                    Dr. Johan Dubbeldam,               TU Delft
                    Massimo Achterberg                 TU Delft, daily supervisor

An electronic version of this thesis is available at `http://repository.tudelft.nl/`.

**TU**Delft

# Abstract

The spreading process of diseases has been an important research topic for many years. It has profound effects on the development of human social behaviors. The underlying social network structure may change when individuals change their connection with other individuals in response to the epidemic. The classic susceptible-infected-susceptible (SIS) model is used to model the spread of an epidemic on a network, where all individuals are defined as nodes and the connections between the individuals are regarded as links. Besides the typical static network, the structure of the network can be related to the state of nodes (infected or susceptible) by link breaking and link creation processes. So the extended network, adaptive susceptible-infected-susceptible model (ASIS model) can be derived.

To study the spreading process on static networks and adaptive networks, we use stochastic simulations and mean field approximations. We assume that the spreading process over the network is a continuous-time discrete-state Markov process. But most recent works use the discrete-time simulator, which is actually an approximation of the process. In this report, we extend a existing continuous-time simulator towards adaptive networks. This existing simulator is based on the Gillespie algorithm. We perform the simulations using both discrete-time Markov chain and continuous-time Markov process. And based on the simulation results, we demonstrate that the continuous-time simulator has a better performance than the discrete-time simulator on modeling both static SIS network and ASIS network with high accuracy.

The second part of this work aims to study the characteristics of the ASIS network in the metastable state. We observe three possible states of the ASIS network: the endemic state, disease-free state and bistable state. The degree distribution of the graph follows a binomial distribution in some cases. By plenty of simulations with different parameters, we illustrate under what circumstances the degree distribution follows the binomial distribution.

# Preface

With this thesis project, *Spreading Processes over Adaptive Networks,* I finished the Master of Science degree in Electrical Engineering at the Delft University of Technology. This project has been carried out at the Network Architectures and Services (NAS) group. I would like to express gratitude to my supervisor Professor Piet Van Mieghem for providing me this opportunity to do research on this topic. I am also grateful for his comments during the mid-term presentation.

I would like to thank Massimo Achterberg, my daily supervisor, for his support and suggestions through out the whole process of this thesis. We had meeting weekly, which was extremely helpful on solving my questions. It was very pleasant to work with Massimo in the past nine months. I also would like to thank Long Ma, as my supervisor of the extra project in three months. His suggestions helped me a lot. And I would like to thank Fenghua Wang for the information about the continuous-time simulator. It is truly my pleasure to work with them.

I would like to thank Dr. Johan Dubbeldam for being a part of my thesis committee.

Finally, I really appreciate my parents for supporting me with love and understanding. And I would like to thank my friends Yanbin He and Maosheng Yang for accompany and encouragement during this tough COVID-19 period.

*Tian Gan*
*Delft, November 2021*

# Contents

# 1

# Introduction

It is declared by the World Health Organization (WHO) that the Coronavirus disease 2019 (COVID-19), which is caused by severe acute respiratory syndrome coronavirus 2 (SARS-CoV-2), is a global pandemic since early 2020 [8]. Due to the huge impacts of COVID-19 on people's daily life and the economy, various works attempt to find out the spreading mechanism of COVID-19 and predict how long the pandemic will last and how many people will be finally affected or deceased [23]. Various other diseases, e.g., the **Plague**, caused millions of victims across many centuries. Consequently, it is vital to investigate how the disease will interact with humanity.

Among all the tools, one typical and basic way to mathematically investigate the dynamics of the spreading disease is first introduced by Kermack and McKendrick [15], where the population is divided into several compartments, and hence the model is called a compartmental model. The compartmental models in epidemiology assume that the population is well-mixed and each individual follows the same connection pattern. One of the most well-known compartmental models is the Susceptible-Infected-Removed (SIR) model [4, 21, 22, 26]. In this model, there is a compartment (group) of healthy and susceptible people (S), a group of people who are infected with the disease and can spread it to susceptible (I) and a group who have been removed (R), i.e., dead. The R compartment may also include the recovered people, who are immune to the disease. It has been proved that the SIR model can accurately model some diseases, such as measles [14].

Another related model is called the Susceptible-Infected-Susceptible (SIS) model. In the SIS model [5], there are two compartments: the fraction of susceptible individuals (S) and the active infectious individuals (I), where the susceptible people can be potentially infected by the infected people. After people cure from the disease, they return to the susceptible state, meaning that they can be infected again. These two models are the foundation of the epidemiological modelling, and plenty of variants are derived from them, e.g., the SIRS model [24].

However, the main drawback of the aforementioned model is that the connection status between individuals is not taken into account. This could be a severe problem when the local topology information takes effect when considering the disease spreading process. To tackle this limitation, agent-based models have been put forward and investigated, where every individual is considered as a node within a network. Furthermore, the connections between the individuals can be modelled as the links or the edges of the network. In this model, each individual is again labelled as susceptible or infected, indicating their health statuses. The infection or the cure process can be modelled as the stochastic process with

probability [29]. Furthermore, the infection process requires the existence of the contact, which utilizes the local topology information of the network in modelling the spreading epidemics. This model through contact networks is called *network epidemiology* [7, 12, 13, 16].

Many models in network epidemiology consider static underlying contact networks, but which are actually changing over time. For example, during the COVID-19 pandemic, usually the infected individuals are asked to stay at home (self-isolation) or are quarantined [27], which basically reduces the number of contacts in the network. This situation is reflected as variation in the network structure. Furthermore, this also illustrates the interaction between the disease and the network itself. Under these circumstances, Gross et al. [11] put forward a new model, where the network is adaptive to the statuses of individuals. This model is named *adaptive network*. In this model, the connection between infected individuals and susceptible individuals can be broken to prevent the spreading of the disease, which has a profound impact on the emerging network [11].

In this thesis, we comprehensively investigate the properties of the adaptive SIS network through many simulations, including the epidemic threshold, metastable prevalence, number of components within the network, assortativity, degree distribution, and so on. Furthermore, many previous simulation results are derived using the discrete-time simulator [3] while the modelled process is actually a continuous stochastic process. It is unknown whether the discrete-time approximation simulation methods is accurate or not. Therefore, in this thesis work, we adapted a continuous time simulator for adaptive network using the Gillespie algorithm. Based on this simulator, we discuss the deviations between the discrete-time and continuous-time simulation results.

This thesis work is organized as follows:

- Chapter 1-Introduction: In this chapter, we first introduce the background and then motivate the research problem of this thesis work.

- Chapter 2-Background: In this chapter, we provide the preliminary knowledge for the thesis work, e.g., the SIS model and the adaptive SIS network, the master equations and its mean-field approximation.

- Chapter 3-Discrete time simulations: In this chapter, based on the simulation results derived by the discrete-time simulator, we provide the definitions of a few important concepts, e.g., metastable prevalence and epidemic threshold. Besides, we also motivate the implementation of SIS network by introducing self infection process.

- Chapter 4-Continuous time simulations: In this chapter, we introduce our continuous time simulator by first discussing the Gillespie algorithm. After that, the implementation of the devised continuous-time simulator is explained and finally, the comparison between the discrete-time simulator and the continuous-time simulator is discussed.

- Chapter 5-Numerical results and discussions: In this chapter, we research on the bistability of the ASIS network and try to find the transitions between three different states of the ASIS network in the metastable state. Besides, we also research the characteristics of metastable topology whereby we focus on the degree distribution

- Chapter 6-Conclusion: This chapter presents the conclusion of the research work and scope of future work on adaptive networks.

# 2

# Background

## 2.1. Graph Theory

In mathematics, the relationships among objects can be modelled as a non-Euclidean mathematical structure, i.e., graph. Let us consider a population of $N$ individuals. Each individual may have connections to other individuals. All individuals can be denoted as nodes or vertices and the connections in between are regarded as links or edges. Then a network can be modelled as a graph $\mathcal{G} = (\mathcal{N}, \mathcal{L})$, where $\mathcal{N}$ is the set of vertices and $\mathcal{L}$ is the set of links [30]. Furthermore, we define $L = |\mathcal{L}|$ and $N = |\mathcal{N}|$. The graph $\mathcal{G}$ can be characterized by a symmetric adjacency matrix $\mathbf{A}$. If the graph is simple and has no self-loops, the element $a_{ij} = [\mathbf{A}]_{i,j}$ specifies whether node $i$ and node $j$ are connected or not. We consider the *unweighted* graph, which means the entry of the adjacency matrix $\mathbf{A}$ is binary. Then the entry of the adjacency matrix obeys the following rules

$$a_{ij} = \begin{cases} 0, & \text{if node } i \text{ and } j \text{ are disconnected,} \\ 1, & \text{if node } i \text{ and } j \text{ are connected.} \end{cases}$$

In this thesis work, we consider the simplified situation where if there is a link from $i$ to $j$, then there exists a link from $j$ to $i$. This means the graph is *undirected*. Therefore, the adjacency matrix $\mathbf{A}$ is symmetric. Furthermore, The degree $d_j$ of a node $j$ in the graph $\mathcal{G}$ is the number of neighbors. If the node $j$ is disconnected to the graph, the degree $d_j = 0$. The degree of a graph is defined as the sum of degrees of all nodes within the graph. Since each link belongs to two connected nodes, it can be counted twice when computing the degree of nodes on their terminal. Then the degree of a graph can be formulated as $\sum_{j=1}^{N} d_j = 2L$.

## 2.2. Stochastic Processes

In this thesis, we intend to simulate epidemics on networks in a probabilistic way which urges us to introduce some concepts about stochastic processes. A stochastic process can be defined as a set of random variables $X(t)$, where time $t$ is within a time series $T$. If $T$ is a continuous set, then $X(t)$ is a continuous time stochastic process. If $T$ is a discrete set, then $X[k]$ is a discrete time process where $k$ is the discrete time instant in the set $T$.

### 2.2.1. Poisson Process

The Poisson process with rate $\lambda \geq 0$ is a continuous time stochastic process, also called as homogeneous Poisson process. It can be defined as a counting process, as this process represents the number of random events within the time intervals. The homogeneous Poisson

process has independent increments following the Poisson distribution

$$\Pr[X(t+s) - X(s) = k] = \frac{(\lambda t)^k e^{-\lambda t}}{k!}, \tag{2.1}$$

where $t > 0$, $s \geq 0$, and $k$ is a non-negative integer. The parameter $\lambda$ is interpreted as the rate of random events occurred in a unit of time. Particularly, the number of events in a time interval with any length $t$ is a Poisson random variable with rate $\lambda t$.

### 2.2.2. Markov processes and Markov chains

Markov processes, for which discrete time and continuous time versions exist, are another example of stochastic processes. For a Markov process, the future state of the random variable only depends on its current state, and not on the previous states. If its state space is discrete, it is called a Markov chain. A Markov chain moves states in discrete time steps, called as discrete-time Markov chain (DTMC). If moves continuously through time, it is named as continuous-time Markov chain (CTMC).

In a Markov process, when the system is stationary and will not change anymore, this system is in the so-called steady state. If the process is in a specific state and cannot leave the state, this state is absorbing state. For example, in SIS epidemics, the absorbing state is all individuals in the system are healthy, which is also named the trivial steady state.

## 2.3. Epidemics on Networks

### 2.3.1. The SIS model

The susceptible-infected-susceptible model (SIS model) is widely used to simulate the spreading of infectious diseases [5]. In the basic SIS model, the population of individuals is separated into two classes: susceptible individuals (denoted by $S$) and infected individuals (denoted by $I$). A susceptible individual is vulnerable and can potentially be infected by contacting an infected individual, whereas an infected individual can possibly recover from the disease. A schematic overview in shown in Figure 2.1.
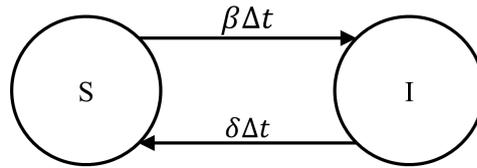


**Figure 2.1:** Transition diagram for the two-state Markov chain of SIS model. $S$ is the susceptible or healthy state, while $I$ is the infectious state.

Here we utilize Bernoulli random variables to describe the state of the individuals. The state of node $i$ at time instant $t$, i.e., $X_i(t) = 1$ when node $i$ is infected at time $t$, whereas $X_i(t)$ is zero when the node $i$ is healthy. During the curing process, infected nodes can recover from the disease. For the infection process, the susceptible nodes can be infected by other infectious nodes. The curing process is a Poisson process with rate $\delta$, while the infection process is a Poisson process with rate $\beta$. We assume that during a small time step $\Delta t$, only one transition occurs in the Markov chain. Conditionally, the infection process can take place on $X_i$ when $X_i$ is healthy, its neighbor $X_j$ is infectious, and node $i$ and $j$

are connected, while the curing process can happen if $X_i$ is infected. Both processes are independent processes. These processes can be formulated as Markov chains,

$$
\begin{aligned}
\text{Infection}: \quad &\Pr[X_i(t+\Delta t)=1|X_i(t)=0, X_j(t)=1, a_{ij}(t)=1] = \beta\Delta t, \\
\text{Curing}: \quad &\Pr[X_i(t+\Delta t)=0|X_i(t)=1] = \delta\Delta t.
\end{aligned}
\tag{2.2}
$$

### 2.3.2. Master equation of SIS model
The master equation of a Markov process is utilized to describe the evolution of the process in the probability of states. To derive the master equations, we first consider a network with two connected nodes. Then the Markov process has two Bernoulli random variables $X_1$, and $X_2$. There are thus $2^2 = 4$ states in total. The possible states of both nodes $\Pr(X_1, X_2)$ are:

- $\Pr(0,0)$: both $X_1$ and $X_2$ are healthy,

- $\Pr(0,1)$: $X_1$ is healthy but $X_2$ is infected,

- $\Pr(1,0)$: $X_1$ is infected but $X_2$ is healthy,

- $\Pr(1,1)$: both $X_1$ and $X2$ are infected.

For one transition from one state to another state in time step $\Delta t$, it can be formed as

$$
\Pr[(X_1,X_2)(t+\Delta t)] = \mathbf{P}\cdot\Pr[(X_1,X_2)(t)],
\tag{2.3}
$$

where $\mathbf{P}$ is the transition probability matrix. The probability of all transitions of the states is described by the transition matrix $\mathbf{P}$.

Then the following transition matrix for the 2 connected nodes in SIS model is derived as

$$
\mathbf{P} =
\begin{array}{cccc}
(0,0) & (0,1) & (1,0) & (1,1)
\end{array}
\begin{pmatrix}
1-2\beta\Delta t & \beta\Delta t & \beta\Delta t & 0 \\
\delta\Delta t & 1-(\delta\Delta t+\beta\Delta t) & 0 & \beta\Delta t \\
\delta\Delta t & 0 & 1-(\delta\Delta t+\beta\Delta t) & \beta\Delta t \\
0 & \delta\Delta t & \delta\Delta t & 1-2\delta\Delta t
\end{pmatrix}.
\tag{2.4}
$$

Taking the time step $\Delta t$ to zero, we move from the discrete-time Markov chain to the continuous-time Markov chain, and the transition matrix is denoted by $\tilde{\mathbf{P}}$, rewritten as

$$
\tilde{\mathbf{P}} =
\begin{array}{cccc}
(0,0) & (0,1) & (1,0) & (1,1)
\end{array}
\begin{pmatrix}
-2\beta & \beta & \beta & 0 \\
\delta & 1-(\delta+\beta) & 0 & \beta \\
\delta & 0 & 1-(\delta+\beta) & \beta \\
0 & \delta & \delta & 1-2\delta
\end{pmatrix}.
\tag{2.5}
$$

Based on the transition matrix, we can derive the differential equations of $\Pr(1,1)$ and $\Pr(1,0)$ as follows

$$
\frac{d\Pr(1,1)}{dt} = -2\delta\Pr(1,1) + \beta\Pr(1,0) + \beta\Pr(0,1),
\tag{2.6}
$$

and

$$
\frac{d\Pr(1,0)}{dt} = \beta\Pr(0,0) + \delta\Pr(1,1) - (\delta+\beta)\Pr(1,0).
\tag{2.7}
$$

Combining equation (2.6) and (2.7), the differential equation of the probability that $X_1 = 1$ and the state $X_2$ is undetermined, $\Pr(1,x)$, is

$$
\frac{d\Pr(1,x)}{dt} = \beta\Pr(0,0) + \beta\Pr(0,1) - \delta\Pr(1,1) - \delta\Pr(1,0).
\tag{2.8}
$$

Based on the Bernoulli property $E[X] = 1 \times \Pr[X = 1] + 0 \times \Pr[X = 0] = \Pr[X = 1]$, equation (2.8) is rewritten as

$$
\begin{aligned}
\frac{d}{dt}E[X_1] \quad &= \beta E[(1 - X_1)(1 - X_2)] + \beta[(1 - X_1)X_2] - \delta E[X_1(1 - X_2)] - \delta E[X_1 X_2] \\
&= -\delta E[X_1] + \beta E[(1 - X_1)X_2].
\end{aligned}
\tag{2.9}
$$

Similarly, we have

$$
\frac{d}{dt}E[X_2] = -\delta E[X_2] + \beta E[X_1(1 - X_2)].
\tag{2.10}
$$

And the correlation between $X_1$ and $X_2$ can be derived as well by the following equation

$$
\begin{aligned}
\frac{d}{dt}E[X_1 X_2] \quad &= \frac{d}{dt}\Pr[X_1 X_2 = 1] \\
&= -2\delta \Pr(1,1) + \beta \Pr(1,0) + \beta \Pr(0,1) \\
&= -2\delta E[X_1 X_2] + \beta E[X_1(1 - X_2)] + \beta E[(1 - X_1)X_2] \\
&= -2\delta E[X_1 X_2] + \beta E[X_1 + X_2 - X_1 X_2].
\end{aligned}
\tag{2.11}
$$

In general, for a network with $N$ nodes, the differential equation of the viral state of node $i$ is obtained as

$$
\frac{d}{dt}E[X_i] = -\delta E[X_i] + \beta \sum_{j=1, j \neq i}^{N} E[(1 - X_i)X_j]E[a_{ij}].
\tag{2.12}
$$

Equation (2.12) shows that the infection process can take place on node $i$ if node $i$ is susceptible $X_i = 0$, and at least one of its neighbours $X_j$ is infected $X_j = 1$, whereas the curing process can take place if and only if node $i$ is infected $X_i = 1$.

Since the nodal dynamics are given by differential equation (2.12), the rates of infection process and curing process are linear additive. For instance, a susceptible node surrounded by four infectious nodes, as shown in Figure 2.2, is possibly infected with rate $4\beta$.
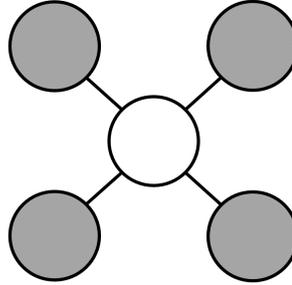


**Figure 2.2:** A five-node network which has a susceptible node (white) surrounded by four infected nodes (gray). Since the rate of infection process is $\beta$ in the SIS model, the center node is infected with total rate $4\beta$.

### 2.3.3. Adaptive SIS model

Links between susceptible and infected individuals are about to be broken to prevent the spreading of epidemics, i.e., self-isolation or quarantine. Besides, susceptible nodes are about to be connected to reduce the disease exposure. Therefore, the structure of the network varies when a link between node $i$ and $j$ is created or broken. Based on this idea, the classical adaptive susceptible-infected-susceptible network model, so-called ASIS model, is established. The ASIS model is first introduced by Gross et al. [11] where a rewiring process to the SIS model is implemented. In this thesis work, the state of a link between node $i$ and $j$ at a certain time instant $t$ is regarded as $a_{ij}(t)$.
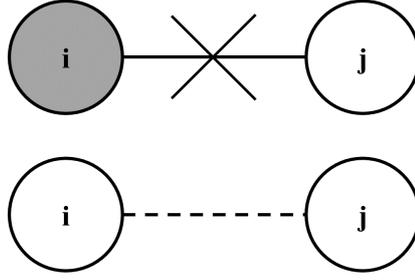
**Figure 2.3:** Schematic overview of two connected nodes. Gray nodes are infected nodes, white nodes are healthy. The link can be broken when $X_i$ is not equal to $X_j$, whereas it can be rewired/created when $X_i = X_j = 0$.

In an adaptive SIS network model, the link-breaking process is a Poisson process with rate $\zeta$. Figure 2.3 shows that it can take place when node $i$ is healthy and the other one $j$ is infected at time $t$ instant or versa. The link-creation process is also a Poisson process with rate $\xi$, which requires both node $i$ and $j$ are healthy, $a_{ij}(t) = 0$ and $a_{ij}(0) = 1$. Then the Markov chains of link-breaking process and link-creation process can be formed as

$$
\begin{aligned}
\text{Link-breaking}: \quad & \Pr(a_{ij}(t+\Delta t) = 0 | X_i(t) \neq X_j(t), a_{ij}(t) = 1, a_{ij}(0) = 1) = \zeta \Delta t, \\
\text{Link-creation}: \quad & \Pr(a_{ij}(t+\Delta t) = 1 | X_i(t) = X_j(t) = 0, a_{ij}(t) = 0, a_{ij}(0) = 1) = \xi \Delta t.
\end{aligned}
\tag{2.13}
$$

With Equation (2.2) and (2.13), this model can be called as adaptive-SIS model, or ASIS model for short.

Going back to our example of the 2-node network, the adaptive SIS model introduces one more random variable $a_{12}$, which describes the existence of a link between node 1 and 2, in addition to the state of nodes, $X_1$ and $X_2$. Then there are $2^3 = 8$ states in total. And the discrete-time transition matrix **P** is formulated as

$$
\begin{array}{cccccccc}
(0,0,0) & (0,0,1) & (0,1,0) & (0,1,1) & (1,0,0) & (1,0,1) & (1,1,0) & (1,1,1)
\end{array}
$$
$$
\begin{pmatrix}
1-\xi\Delta t & \xi\Delta t & 0 & 0 & 0 & 0 & 0 & 0 \\
0 & 1 & 0 & 0 & 0 & 0 & 0 & 0 \\
\delta\Delta t & 0 & 1-\delta\Delta t & 0 & 0 & 0 & 0 & 0 \\
0 & \delta\Delta t & \zeta\Delta t & 1-(\delta+\beta+\zeta)\Delta t & 0 & 0 & 0 & \beta\Delta t \\
\delta\Delta t & 0 & 0 & 0 & 1-\delta\Delta t & 0 & 0 & 0 \\
0 & \delta\Delta t & 0 & 0 & \zeta\Delta t & 1-(\delta+\beta+\zeta)\Delta t & 0 & \beta\Delta t \\
0 & 0 & \delta\Delta t & 0 & \delta\Delta t & 0 & 1-2\delta\Delta t & 0 \\
0 & 0 & 0 & \delta\Delta t & 0 & \delta\Delta t & 0 & 1-2\delta\Delta t
\end{pmatrix}.
$$

### 2.3.4. Master equation of adaptive SIS network

Generally for an adaptive SIS network with $N$ nodes, the differential equation of the state of node $i$ can be derived by equation (2.12), as mentioned in section 2.3.2. The governing equation of the link $a_{ij}$ equals

$$
\frac{d}{dt}E[a_{ij}] = E[-\xi a_{ij}(X_i - X_j)^2 + \zeta(1 - a_{ij})(1 - X_i)(1 - X_j)].
\tag{2.14}
$$

In Equation (2.14), we can see that the link-breaking process with rate $\xi$ can take place on a link between node $i$ and node $j$ if there exists a link $a_{ij}$ in between and node $i$ is

healthy and node $j$ is infected or versa. For the link-creation process, it can happen if and only if both nodes are healthy $X_i = X_j = 0$ and there is no link $a_{ij} = 0$.

To make these equations dimensionless, the parameters are also important in the following investigation

$$\xi^* = \frac{\xi}{\delta}, \zeta^* = \frac{\zeta}{\delta}, \tau = \frac{\beta}{\delta}, \omega = \frac{\zeta}{\xi}, \tag{2.15}$$

where $\tau$ is the effective infection rate and $\omega$ is the effective link-breaking rate. Here we set the curing rate $\delta = 1$ in the simulations, which is the scale of time for the average curing time is equal to the unit of time. In the remainder, we will drop the asterisk * for $\zeta$ and $\xi$.

### 2.3.5. Mean-field differential equations

This mean-field approximation is proposed by Van Mieghem [32], which is called N-interwined mean-field approximation (NIMFA). The mean-field approximation is by taking the following assumption

$$E[XY] = E[X]E[Y], \tag{2.16}$$

for each random variable $X$ and $Y$ in the model. The reason for taking the mean-field approximation is because for larger networks, the mean-field EDEs are the only way to compute the properties of the network [2].

Taking the mean-field approximation into account, there is no correlation between the random variables $X$ and $Y$ [32]. Then the differential equations (2.12) and (2.14) are reformulated as

$$\frac{d}{dt} E[X_i] = -E[X_i] + \tau \sum_{j=1, j \neq i}^{N} (1 - E[X_i]) E[X_j] E[a_{ij}], \tag{2.17}$$

$$\begin{aligned} \frac{d}{dt} E[a_{ij}] = a_{ij}(0)(&-\zeta E[a_{ij}](E[X_i] + E[X_j] - 2E[X_i]E[X_j]) \\ &+ \xi(1 - E[a_{ij}])(1 - E[X_i])(1 - E[X_j])). \end{aligned} \tag{2.18}$$

Specially when $\zeta = \xi = 0$, the ASIS model can be regarded as static SIS model since the number of links in the network does not change, as shown in equation (2.12).

<div align="right" style="font-size:4em">3</div>

# Discrete time simulations

In this thesis, all Markov processes are considered to be continuous time. Thus we have CTMC for the epidemics models. However, in this section, all numerical results are derived by discrete time simulations, which are basic Markov Chain Monte Carlo method. To be specific, we consider that all results modelled by continuous-time simulations are exact, whereas discrete-time simulations are the approximations. In this thesis work, all simulations are performed on a complete network and the initial condition is that all nodes are infected.

## 3.1. Static SIS network

The Monte Carlo simulation of the static SIS Markov process is shown in Figure 3.1. The red curve shows that the fraction of infected nodes declines rapidly and then converges to around 0.8 with oscillations for a period, which is called the endemic state or metastable state [20].

For lower infection rates $\beta$, the fraction of infected nodes will be lower. If $\beta$ is lower than a certain value, the fraction of infected nodes will decrease exponentially to zero. The largest infection rate $\beta$ for which exponential convergence occurs, is called the epidemic threshold.

### 3.1.1. Metastable states

As discussed in the section 2.2.2, the Markov process has a steady state. The SIS Markov process exists a similar state but slightly different. The process might be in this state for a period of time before converging to the steady state. This state is called ***metastable state***, or ***endemic state***. A system can have the metastable state but it always collapses to the trivial steady state when time tends to infinity.

In this thesis work, the average fraction of the infected individuals at a certain time is named the **prevalence** $y$. It can be defined as [1]

$$y = \frac{1}{N} \sum_{i=1}^{N} E(X_i). \tag{3.1}$$

The metastable state, also called endemic state, is a non-zero prevalence $y$ for a large period $T$. Mathematically, it can be derived by

$$y = \frac{1}{NT} \int_0^T \sum_{i=1}^{N} E(X_i(t)) dt. \tag{3.2}$$
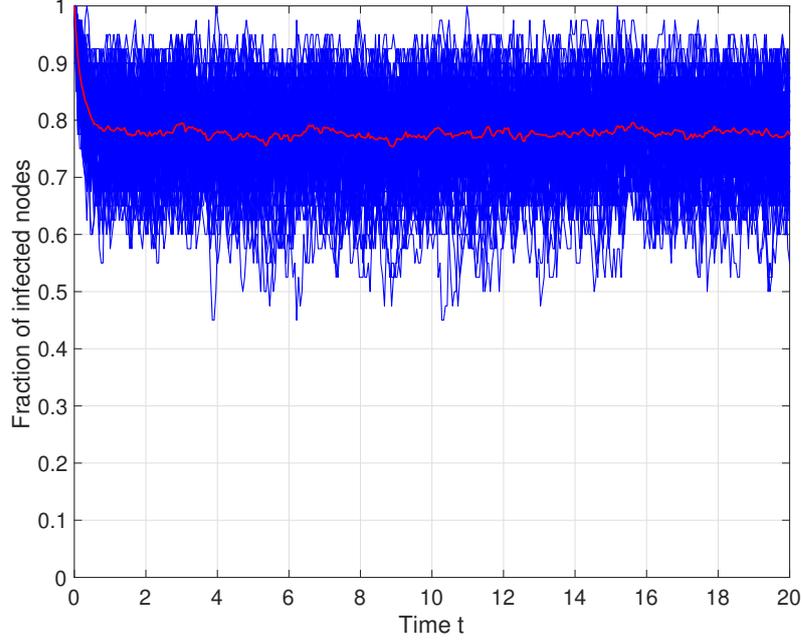
**Figure 3.1:** Simulations derived from 100 runs of the Markov process in the complete static SIS network with size $N = 40, \delta = 1, \beta = 0.125$, and $\Delta t = 0.05$. The red curve is the average prevalence of the 100 runs of the Markov process. The underlying graph is the complete graph and initially all nodes are infected.

For example, in Figure 3.2, when time $t$ is very large, the prevalence $y$ tends to die out, where the process is in the absorbing state. Before the absorbing state, the prevalence $y$ stays to a non-zero state for a long period, where the state is the endemic state.

### 3.1.2. Epidemic threshold $\tau_c$ of static SIS model

Theoretically, the epidemic threshold $\tau_c$ is defined as the largest effective infection rate $\tau$ with a non-zero fraction of infected nodes in the endemic state [32]. In an SIS network, the stochastic epidemic threshold $\tau_c$ is lower bounded by the epidemic threshold $\tau_c^{(1)}$ from mean-field approximation [32]

$$\tau_c \geq \tau_c^{(1)} = \frac{1}{\lambda_1}, \tag{3.3}$$

where $\lambda_1$ is the largest eigenvalue of the adjacency matrix **A**.

Thus in the $N$-size complete static SIS network $K_N$, the mean-field epidemic threshold

$$\tau_c^{(1)} = \frac{1}{d} = \frac{1}{N-1}, \tag{3.4}$$

where $d$ indicates the degree of the network.

For various effective infection rate $\tau$, the Markov processes of the SIS network are shown in Figure 3.3. For $\tau = 0$ which is lower than $\tau_c$, the Figure 3.3 shows that the epidemic process exponentially dies out because the effective infection rate $\tau$ is smaller than the epidemic threshold $\tau_c$. When $\tau > \tau_c$, the prevalence $y$ will converge to an non-zero value for the prevalence y, which corresponds to the endemic state.
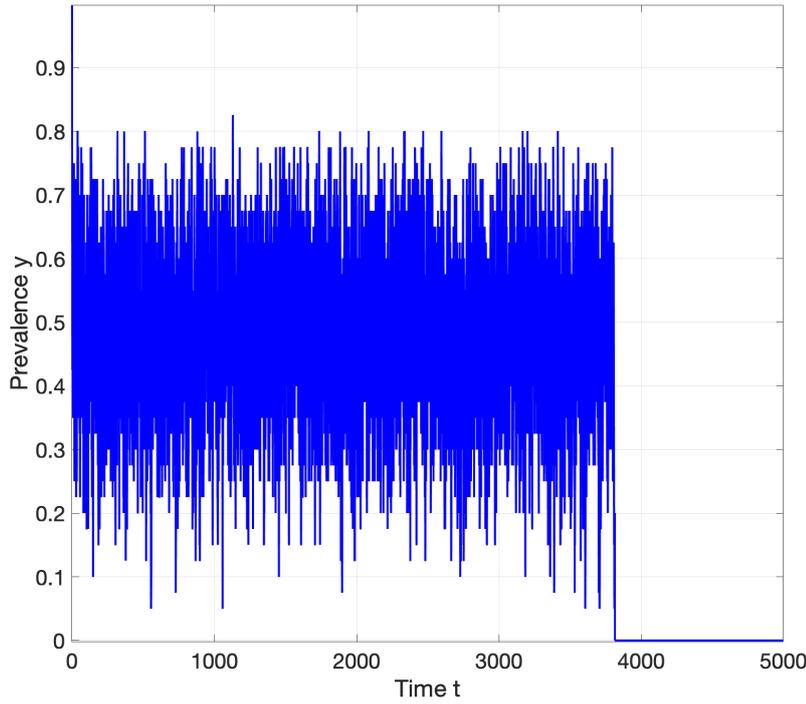
**Figure 3.2:** A single run of a complete static SIS network with size $N = 40$, $\delta = 1$, $\beta = 0.05$, and $\Delta t = 0.05$. The simulation period is 100,000 time units.
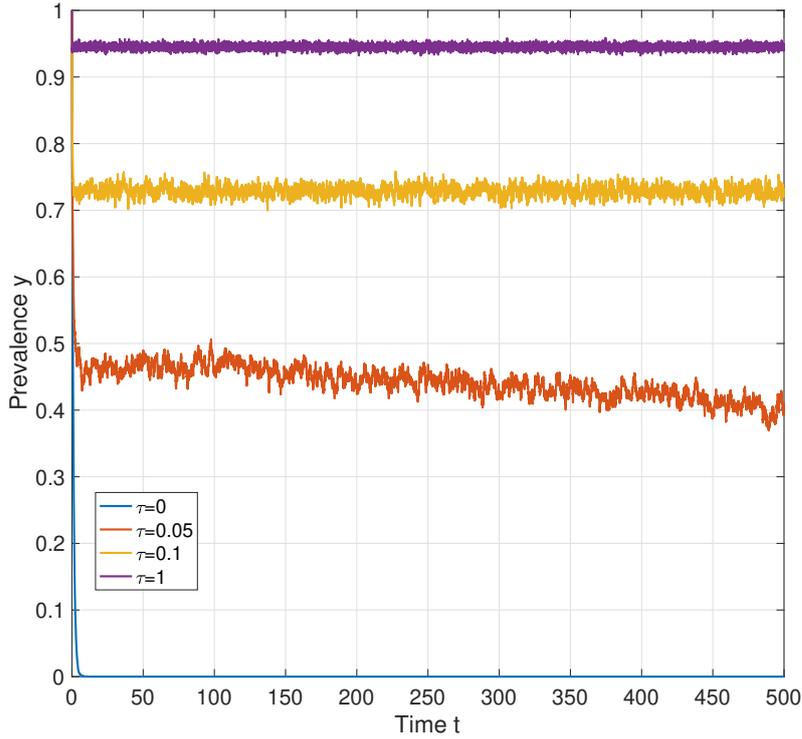
## 3.2. $\epsilon$ -SIS model

### 3.2.1. Metastable prevalence

Since the epidemic of a finite network finally disappears on a sufficiently large timescale, the real steady state of SIS model with $\epsilon = 0$ on any finite graph is the absorbing state. It is difficult to determine the epidemic threshold accurately. To prevent this situation and to investigate the metastable state of infected nodes, a self-infection rate $\epsilon$ is introduced to simulate the so-called $\epsilon$-SIS model [31]. When the self-infection rate $\epsilon < \frac{\delta}{N}$, any healthy node can infect itself with a very small probability. Furthermore, the self-infection is also called external infections, for example, by contaminated surfaces, bacteria, etc. Thus self infection process is independent of infection process and curing process in $\epsilon$-SIS model. In Figure 3.4, since there are only self infection process and curing process in this case, and both self-infection rate $\epsilon$ and curing rate $\delta$ are the same, the prevalence $y$ in this SIS model finally converges to 50 percent.

Therefore, introducing self-infection process is an approach to research the metastable state [31]. The relation between the metastable prevalence $y$ and various effective infection rates $\tau$ on a complete SIS network is shown in Figure 3.5.

We take 10,000 time units for one simulation and 100 simulations for one event. Then the relation between the metastable prevalence $y$ and the effective infection rate $\tau$ is shown in Figure 3.5. The metastable prevalence $y$ start to increase with relatively larger value of $\tau$. The epidemic threshold $\tau_c$ can be estimated here at $\tau_c \approx 0.023$. For the values of effective infection rate $\tau$ which are below the estimated epidemic threshold $\tau_c$, the epidemics are difficult to spread over the $\epsilon$-SIS model.

**Figure 3.3:** Simulations for the complete static SIS network with size $N = 40$, $\delta = 1$, and $\Delta t = 0.05$. The effective infection rate $\tau$ is set as 0, 0.05, 0.1, 1, respectively. For an SIS network with $N = 40$ nodes, the mean-field epidemic threshold $\tau_c^{(1)} = \frac{1}{39} \approx 0.0256$.

## 3.3. $\epsilon$-ASIS model

Introducing the link-breaking process and link-creation process to extend the $\epsilon$-SIS model, this network model is named as adaptive $\epsilon$-SIS model (or $\epsilon$-ASIS model). A single run of the $\epsilon$-ASIS model is shown in Figure 3.6, in which the initial network is a complete graph. It shows that the number of links decreases corresponding to the increasing number of infected nodes.

Because of the network adaptation, the prevalence of adaptive SIS network has larger oscillations than the prevalence of the static SIS model in the metastable state. As shown in Figure 3.6(a), the average steady-state number of infected nodes is around the fluctuated number of infected nodes.

### 3.3.1. Epidemic reemergence

Introducing the self infection rate $\epsilon$ to the ASIS network, we can observe the phenomenon of epidemic reemergence that the prevalence $y$ stays at a low level for a long time, then suddenly surges to a high level before decreasing to a low level again [35]. This process may repeat for several times. As shown in Figure 3.7 where the infection rate $\tau = 0.1$ which is lower than epidemic threshold $\tau_c$, the prevalence $y$ drops to zero for a period of time, and suddenly increase rapidly, and then drops to zero again.

Once the disease invades a giant component within a network, the infection may quickly spread over the whole component, leading to a large number of infected nodes in the giant component. Furthermore, when nodes get infected, this component quickly breaks into
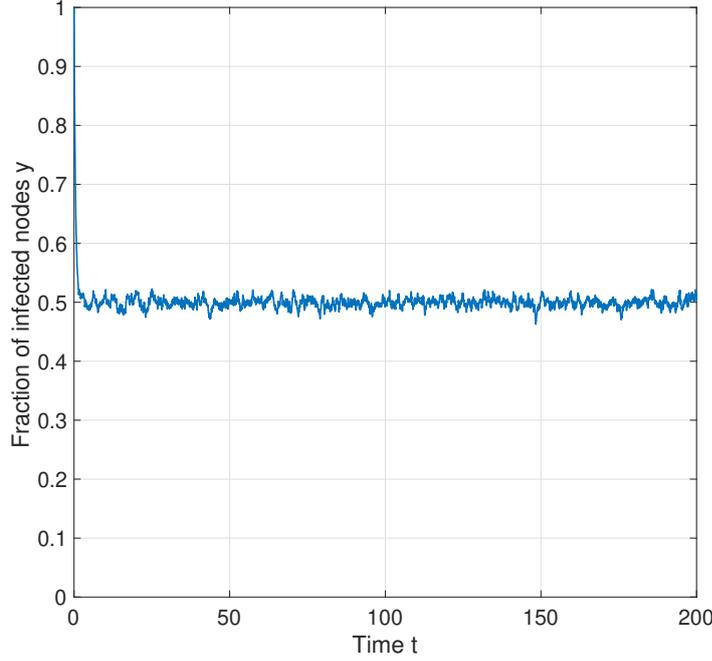
**Figure 3.4:** *Example*: A single run of the Markov process of the static SIS network with $\tau = 0$, $\epsilon = \delta = 1$. The simulation period is 4,000 time units. Only self infection process and curing process can take place in this model.

small pieces due to the link removals. This can be evidenced by the increasing number of components and decreasing size of the giant component. This mechanism is how the adaptive system prevents the epidemic spreading. Figure 3.8 shows the topology structures of the ASIS network in Figure 3.7 at time unit $t = 99$ and $t = 100$, respectively. It is observed that one node in the largest component get self infection in Figure 3.8(a). Then the infection spread over the whole component, while the links between these infected nodes and the rest healthy nodes are quickly disconnected, as shown in Figure 3.8(b).

### 3.3.2. Epidemic threshold $\tau_c$ of $\epsilon$-ASIS model

In an ASIS network, the stochastic epidemic threshold $\tau_c$ is lower bounded by the mean-field epidemic threshold since the mean-field approximation seems to overestimate the Markov process.

Based on the property of the link dynamics, the infected nodes tend to be isolated so as to prevent the spreading of epidemics. Therefore, the infectious disease in the $\epsilon$-ASIS model has a higher possibility to die out, even when $\tau$ is small. After adding the link-dynamic processes to the $\epsilon$-SIS model, the epidemic threshold $\tau_c$ of the $\epsilon$-ASIS model increases compared to the $\epsilon$-SIS model.

Furthermore, to investigate the characteristics of $\tau_c$ on $\epsilon$-ASIS model, we choose the effective link-breaking rate $\omega$ as 1 and 2 with various effective infection rate $\tau$ from 0 to 0.3. In Figure 3.9, the epidemic threshold $\tau_c$ increases with the increasing effective link-breaking rate $\omega$. With larger effective link-breaking rate, more links in the model tend to be broken when the state of nodes and links satisfy the link-breaking rule. Then more nodes are more possible to be susceptible or healthy so that impacts on the spreading of epidemics. As in-
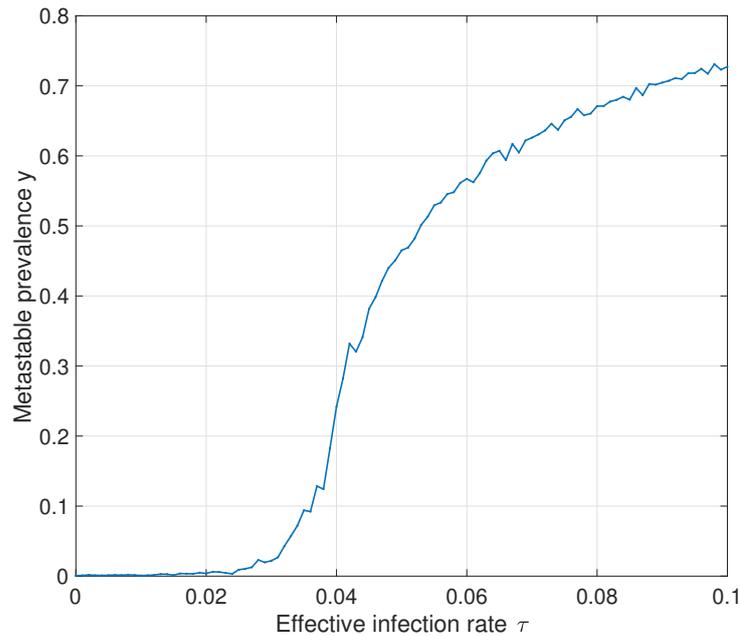
**Figure 3.5:** The relation between the metastable prevalence $y$ and the effective infection rate $\tau$ in the complete static SIS network with size $N = 40$, $\delta = 1$, $\epsilon = 0.001$, and $\Delta t = 0.05$. The epidemic threshold $\tau_c$ can be estimated here at $\tau_c \approx 0.023$. The simulation period is 10,000 time units. The results are averaged over 100 simulations.

dicated by simulation results in Figure 3.9, the epidemic threshold $\tau_c$ of the $\epsilon$-ASIS model tends to be larger for which the effective link-breaking rate $\omega$ is larger.

For the initial complete $\epsilon$-ASIS network with all infected nodes, when the infection rate $\tau$ is smaller than or close to the effective infection rate $\tau_c$, the number of links decreases rapidly from the beginning, and then goes up again and finally converges to the metastable state, whereas the number of infected nodes drops down to the metastable state. A example is shown in Figure 3.10. Since all nodes are infected at the beginning, these infected nodes could be cured. During the curing process, the link-breaking process could take place with the increasing number of healthy nodes. After a period, the link creation process could take place because of many existing pairs of unconnected and healthy nodes.
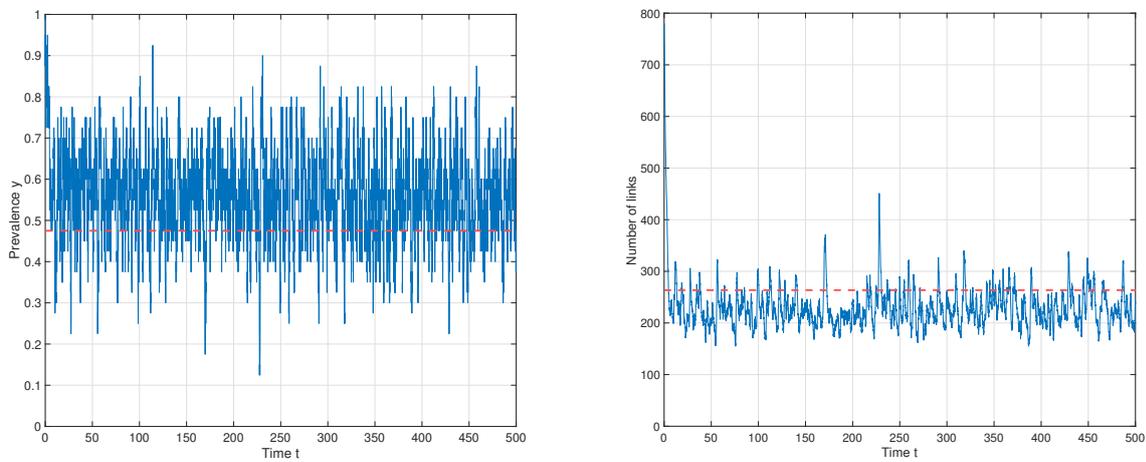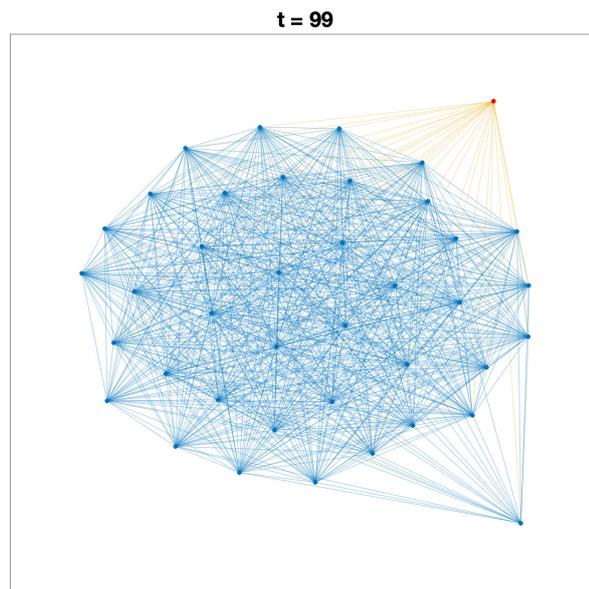
**(a)** Prevalence of number of infected nodes        **(b)** Prevalence of number of links

**Figure 3.6:** A single run of Markov process for the adaptive $\epsilon$-SIS network which is initially the complete graph, with $N = 40$, $\epsilon = 10^{-3}$, $\beta = 0.25$, $\zeta = \xi = \delta = 1$. The red dashed line is the average of the steady state.
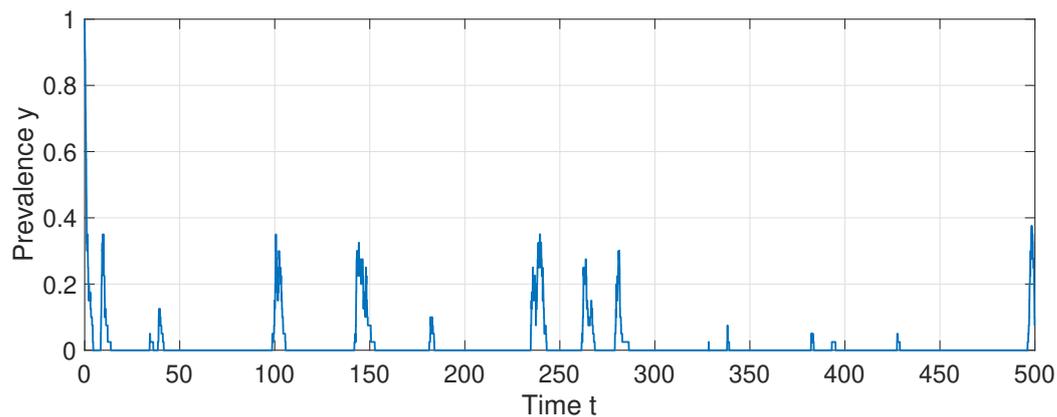


**Figure 3.7:** A single run of the Markov process of the ASIS network with size $N = 40$, $\tau = 0.1$, $\omega = 2$, $\epsilon = 0.001$.

**(a)** Graph of ASIS network with one infected node
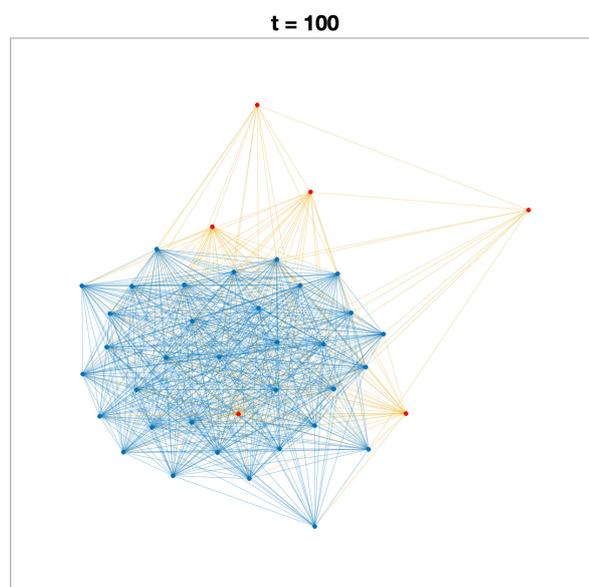


**(b)** Graph of ASIS network after disease spreading

**Figure 3.8:** Snapshots of topology structures of ASIS network in Figure 3.7. (a) Graph of the ASIS network at $t = 99$; (b) Graph of the ASIS network at $t = 100$. Blue nodes are healthy nodes, while red nodes are infected. Yellow links shows S-I links in the topology.
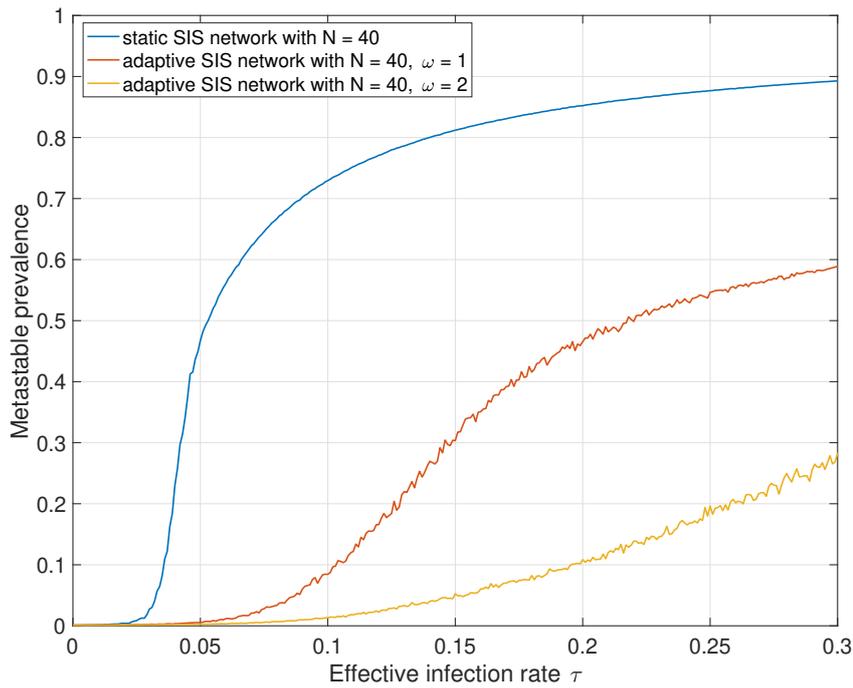
**Figure 3.9:** Comparison the relations between metastable prevalence $y$ and the effective infection rate $\tau$ on both $\epsilon$-SIS model and $\epsilon$-ASIS model. Here we set $\delta = \xi = 1$, and $\epsilon = 0.001$. Both two models are initially complete graph. The epidemic threshold of $\epsilon$-SIS model can be estimated as around 0.03. The epidemic threshold of $\epsilon$-ASIS model with $\omega = 1$ is approximately 0.05, and $\epsilon$-ASIS model with $\omega = 2$ is around 0.07.
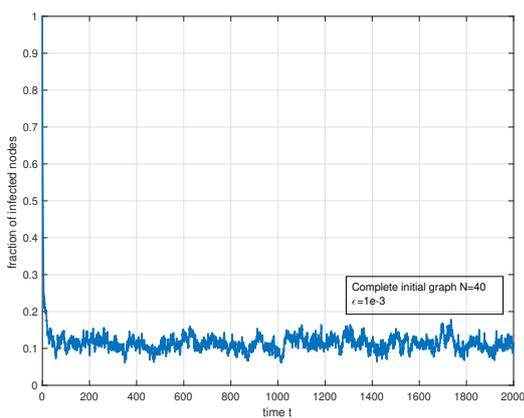


**(a)** Prevalence of number of links
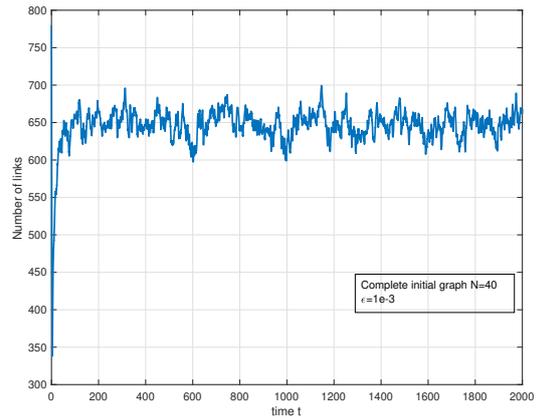


**(b)** Prevalence of number of infected nodes

**Figure 3.10:** A single run of Markov process for the adaptive $\epsilon$-SIS network which is initially complete, with $N = 40, \epsilon = 10^{-3}, \omega = 1, \tau = 0.1$. The simulation period is 400,000 time units.

# 4

# Continuous time simulations

In this chapter, we will discuss the continuous-time simulation method, i.e., Gillespie algorithm, to simulate the epidemics spreading process. Since the discrete-time simulations were approximations of continuous-time processes, just using the discrete-time simulator might introduce (large) errors in the results. As the core of the devised simulation method, the implementation of Gillespie algorithm will be introduced in the following section first. Then the continuous simulator is described in the form of pseudo code.

## 4.1. Gillespie Algorithm

The Gillespie algorithm was introduced by Daniel Gillespie to first simulate the chemical or biochemical system of reactions with high efficiency. It can produce a statistically correct solution of a stochastic equation where the reaction rate is known [9, 10]. Furthermore, this algorithm is introduced to simulate processes on networks as well [18, 33]. In this thesis, the Poisson process is attached to each node and link and the rate of the Poisson process changes according to the status of the network. The most direct and simplest way to simulate the process over such networks is to discretize time, which has been described and implemented in the previous sections. However, this method is suboptimal [18] and the length of the time interval $\Delta t$ has to be sufficiently small to obtain results with high accuracy. As a comparison with the discrete-time implementation, we will utilize the Gillespie algorithm to simulate the stochastic processes over the networks.

### 4.1.1. Pseudo code

In this section, we will first explain the main idea of the Gillespie algorithm and then provide the implementation in pseudo code.

The original Gillespie algorithm considers $N$ independent Poisson processes with rate $\lambda_i$ ($1 \leq i \leq N$). The main idea of the Gillespie algorithm consists of two steps. In the first step, a time increment $\Delta t$ to the next event is determined by the superposition of all $N$ Poisson processes. The waiting time between two consecutive transitions is exponentially distributed. Since these processes are independent, the process describing the event occurring is also Poisson distributed, and the corresponding rate is the sum over all the rates. In the second step, we have to determine one process from all the $N$ possible events that produce this event according to the probability defined as follows

$$\Pi_i = \frac{\lambda_i}{\sum_{j=1}^{N} \lambda_j}.$$ 

(4.1)

Miller and Ting have developed a Python tool for simulating Markovian SIS and SIR epidemic processes on the static network, which is available here [19]. We extend the current tool for adaptive networks. The main idea of the Gillespie algorithm for the adaptive $\epsilon$-SIS ($\epsilon$-ASIS) network has four iterations steps as follow.

1. Find the rate of all possible events including nodal dynamics and link dynamics, and compute the total rate, which is determined by the superposition of all the Poisson processes; the events are the changes of node or link statuses; it could be infected node get recovered, at-risk susceptible node get infected, and a link is broken or created;

2. Based on this rate of change, select the waiting time until the next event from an exponential distribution whose rate is the total rate of change;

3. Select which event takes place, with its probability proportional to the rate of each event;

4. Apply the changes for the event to the current system and repeat from step 1.

We provide a more detailed pseudocode of the Gillespie algorithm in Algorithm 1.

## 4.2. Continuous-time method vs. discrete-time method

### 4.2.1. Case study 1: comparison of prevalence on the static and adaptive SIS network

To investigate the difference between the continuous-time simulations and discrete-time simulations, we implement both methods on a static SIS network and an adaptive SIS network with specific parameters. We perform 10,000 simulations for each model and compare their average prevalence. The comparison results are shown in Figure 4.1.

In Figure 4.1a, we compare the difference between discrete-time simulations and continuous-time simulations. It shows that the prevalence $y$ of the discrete-time simulation has a lower convergence in the metastable state than that of the continuous-time simulation. In Figure 4.1b, we can see that the discrete-time simulations on adaptive SIS network also have deviation with the results from continuous-time method.

### 4.2.2. Case study 2: comparison on static SIS network with various $\tau$

In this section, we compare the continuous-time method and discrete-time method by simulating the static SIS model with different $\tau$ values. The results are shown in Figure 4.2, where the static SIS network is a complete graph with size $N = 40$. For the relation between the metastable prevalence and the effective infection rate $\tau$, the simulation results from discrete-time method with $\Delta t = 0.01$ is close to the result of continuous-time simulations, whereas the results from discrete-time method with $\Delta t = 0.05$ has more deviation, which means that with smaller $\Delta t$ the simulation results would be more accurate.

In terms of the computation time, the Figure 4.2b shows that the discrete-time method with $\Delta t = 0.01$ runs much longer than the continuous-time method. It also shows that one discrete-time simulation with a larger time step requires longer time to operate. Besides, we can observe that when the effective infection rate $\tau$ is below the epidemic threshold $\tau_c$ in the static SIS model, the run time is small. For $\tau > \tau_c$, the run time and metastable prevalence of simulations increase when $\tau$ increases. But for $\tau > 0.05$, we can see that the run time of discrete-time simulations starts to decrease but the continuous-time simulations show opposite behaviour.

Since it is difficult to spread epidemic over the static SIS network when $\tau < \tau_c$, it is merely to operate both infection process and curing process, which are described by Equation

---

**Algorithm 1** Gillespie Algorithm for $\epsilon$-ASIS network

---

**Data:** Graph $G$, transmission rate per edge $\tau$, recovery rate $\delta$, self infection rate $\epsilon$, link breaking rate $\zeta$, link creation rate $\xi$, set of index nodes initial_infecteds, maximum time period $T$

**Result:** Lists of times $t$, number of susceptible nodes at each time $S$, number of infected nodes at each time $I$, number of links at each time $L$.

1  **Initialization**: times t, S, I, L ← [0],[|$G$|-#initial_infecteds], [#(initial_infecteds)], [#($G.edges$)]

2  infected_nodes ← initial_infecteds

3  susceptible_nodes ←[|$G$|- initial_infecteds

4  **for** *infected_node in infected_nodes* **do**

5     | **for** *node in G.nodes* **do**

6     |   | **if** *status[node] is susceptible* **then**

7     |   |   | add (infected_node, node) to IS_links /* IS_links are the list of the possible pairs of infected node and susceptible node */

8     |   | **end**

9     | **end**

10  **end**

11  **for** *susceptible_node in susceptible_nodes* **do**

12     | **for** *node in G.nodes* **do**

13     |   | **if** *status[node] is susceptible* **then**

14     |   |   | add (susceptible_node, node) and (node,susceptible_node) to SS_links /* SS_links are the list of the possible pairs of susceptible node and susceptible node */

15     |   | **end**

16     | **end**

17  **end**

18  IS_edge ← list of the actual I-S edges configured in $G$

19  SS_edge ← list of the S-S edges not existed in $G$

20  total_transmission_rate ← $\tau$ × IS_edge

21  total_recovery_rate ← $\delta$ × infected_nodes

22  self_infection_rate ← $\epsilon$ × S

23  total_nodal_rate ← total_transmission_rate + total_recovery_rate + self_infection_rate

24  total_link_breaking_rate ← $\zeta$ × IS_edge

25  total_link_creation_rate ← $\xi$ × SS_edge ×0.5

26  total_adaptive_rate ← total_link_breaking_rate + total_link_creation_rate

27  total_rate = total_nodal_rate+total_adaptive_rate

28  time ← exponential_variate(total_rate)

29  **while** *time < T* **do**

30     | Execute Iteration Algorithm 2

31  **end**

32  **return** times, $S$, $I$, $L$

---

---

**Algorithm 2** Iteration

---

$r$ = uniform_random(0, total_rate)
**if** $r <$ *total_nodal_rate* **then**
    *r_nodal* = uniform_random(0,total_nodal_rate)
    **if** r_nodal $<$ *total_recovery_rate* **then**
        /* Curing process */
        $u$ = random.choice(infected_nodes)
        remove $u$ from infected_nodes
        add $u$ to susceptible_nodes
        **for** *node in G.nodes* **do**
            **if** *status[node] is susceptible* **then**
                remove ($u$,node) from IS_links
                add ($u$,node) and (node,$u$) to SS_links
            **else**
                add (node,$u$) to IS_links
            **end**
        **end**
        update times, *S*, *I*, *L*
    **end**
    *r_infect* = uniform_random(0,total_transmission_rate+self_infection_rate)
    **if** r_infect $<$ *total_transmission_rate* **then**
        /* Infection process */
        random choose (transmitter, recipient) from IS_edge
        remove recipient from susceptible_nodes
        add recipient to infected_nodes
        **for** *node in G.nodes* **do**
            **if** *status[node] is susceptible* **then**
                add (recipient,node) from IS_links
                remove (recipient,node) and (node,recipient) to SS_links
            **else**
                remove (node,recipient) to IS_links
            **end**
        **end**
        update times, *S*, *I*, *L*
    **end**
    /* Self infection process */
    **for** *node in G.nodes* **do**
        random remove $u$ from susceptible_nodes
        add $u$ to infected_nodes
        **if** *status[node] is susceptible* **then**
            add ($u$,node) to IS_links
            remove ($u$,node) and (node,$u$) from SS_links
        **else**
            remove (node,$u$) to IS_links
        **end**
    **end**
    update times, *S*, *I*, *L*
**end**
/* Link breaking process */
*r_link* = uniform_random(0,total_adaptive_rate)
**if** r_link$<$*total_link_breaking_rate* **then**
    random choose *edge* from IS_edge
    remove *edge* from *G*
    update times, *S*, *I*, *L*
**else**
    /* Link creation process */
    random choose *edge* from SS_edge
    add *edge* to *G*
    update times, *S*, *I*, *L*
**end**
update IS_edge, SS_edge
update total_recovery_rate,total_transmission_rate,self_infection_rat
update total_link_breaking_rate, total_link_creation_rate
update total_nodal_rate, total_adaptive_rate, and total_rate
time ← time + exponential_variate(total_rate)

---
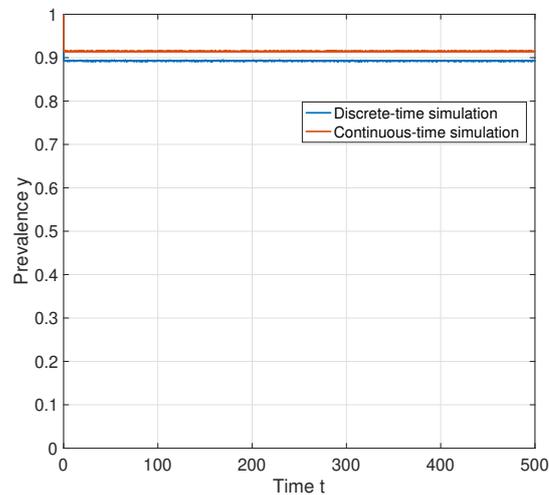
**(a)** Simulations on static SIS network with size $N = 40$, $\tau = 0.3$, $\epsilon = 10^{-3}$, and $\Delta t = 0.05$.
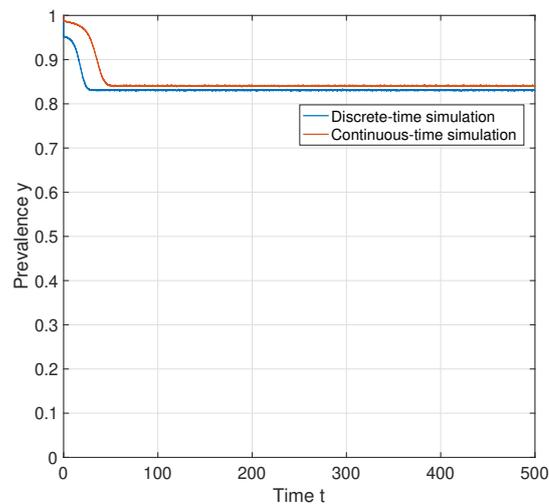


**(b)** Simulations on ASIS network with size $N = 40$, $\tau = 1$, $\omega = 2$, $\epsilon = 10^{-3}$, and $\Delta t = 0.05$.

**Figure 4.1:** Prevalence of static SIS network and adaptive SIS network. The blue curve is simulated by discrete-time method, while the red one is derived by continuous-time method. The simulation period is $10^5$ time units.

(2.2). For the larger $\tau$ above $\tau_c$, there are more infected nodes in the metastable state of the static SIS network because of more operations of Markov processes. But when $\tau$ is very large, the epidemic will spread fast over the network and then less operations of infection processes are required in the discrete-time method. In the continuous-time simulations, the waiting time of each event is based on the total rate of change, which includes transmission rate $\tau$, self infection rate $\epsilon$ and curing rate $\delta$ of the static SIS model. Thus with the increasing $\tau$, the run time of continuous-time simulator increases.

### 4.2.3. Case study 3: comparison on adaptive SIS network with various $\tau$

In this section, we compare both continuous-time simulator and discrete-time method by simulating the adaptive SIS network with various $\tau$. In Figure 4.3a, the discrete-time simulation with $\Delta t = 0.05$ is very different compared to the continuous-time simulations and the discrete-time simulation with $\Delta t = 0.01$, leading to the same conclusion in the previous case, which is when $\Delta t$ becomes smaller, then the deviation between two models are smaller as well. Figure 4.3b shows that in the case of discrete-time simulation, with smaller $\Delta t$, more time is required by the simulation. In terms of the continuous time simulation, at first, it requires a little time but when the $\tau$ becomes larger, the required amount of time increases as well.

For $\tau$ below $\tau_c$, there is no practically spreading process on the adaptive SIS network. That is the reason why the continuous-time simulator runs so fast for the small $\tau$. When $\tau$ becomes larger and larger, since the length of the time interval between two consecutive transitions is generated using the exponential distribution, if the rate is larger, then the time interval is shorter on average. More operations are required if the total length of the time period remains constant. This is the reason why the run time increases with the increase of $\tau$. In contrast, the required run time for discrete-time simulation only changes slightly. This might be due to the adaptiveness of the network topology.

## 4.3. Summary

In this chapter, we first demonstrate the continuous-time simulator based on the Gillespie algorithm and then compare the simulation results derived from the discrete-time and continuous-time simulators. By observing the simulations, we can conclude that, first, when the $\Delta t$ becomes smaller and smaller, then the deviation between the discrete-time simulator and continuous-time simulator becomes smaller as well. Then the continuous-time simulator would consume more time when the value of the parameters is large. It is because this simulator is implemented by an event-driven algorithm. The increasing value of the parameters would increase the number of events take place. Thus there is a trade-off between accuracy and time consumption.
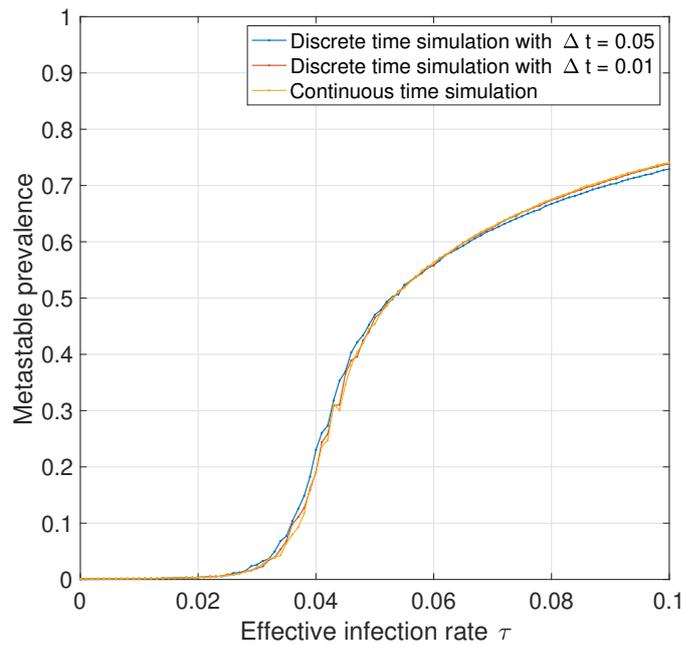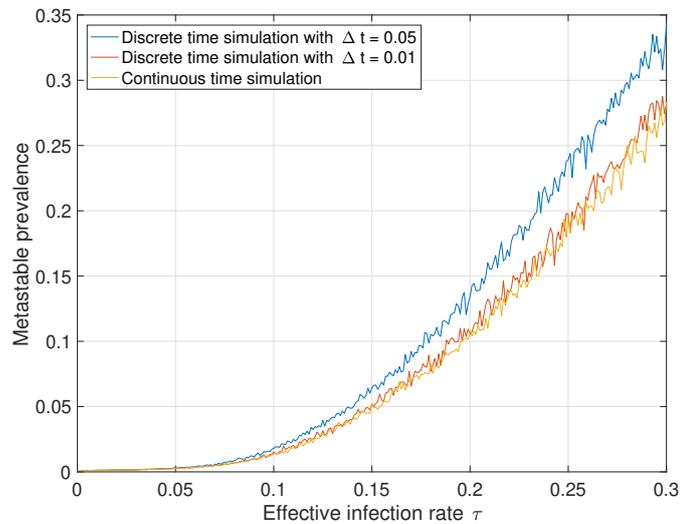
**(a)** Relations between metastable prevalence and effective infection rate $\tau$ on continuous-time simulations and discrete-time simulations of static SIS network.
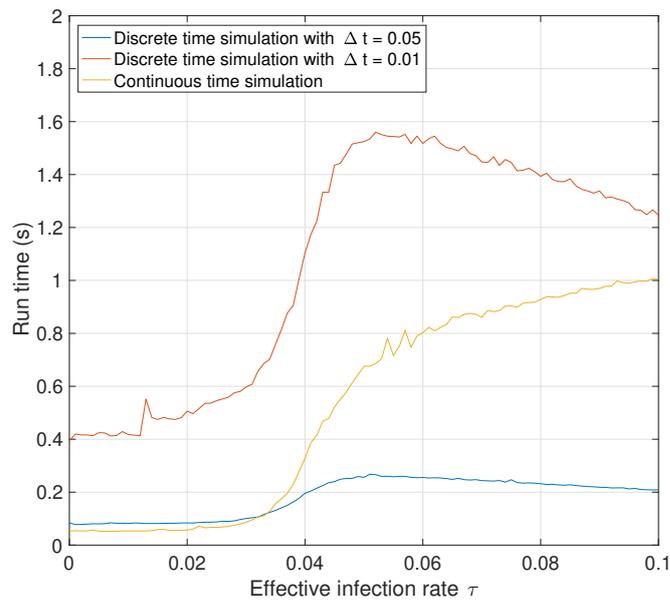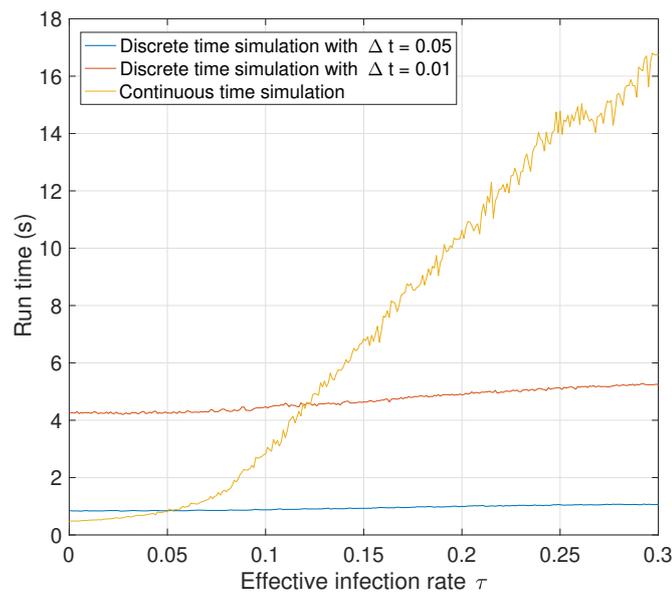


**(b)** Relations between averaged computation time and effective infection rate $\tau$ on continuous-time simulations and discrete-time simulations of static SIS network.

**Figure 4.2:** Continuous-time simulations and discrete-time simulations on static SIS network with size $N = 40$, $\epsilon = 0.001$. Effective infection rate $\tau$ is in range of $(0, 0.1)$, and time period $T = 500$. The blue curve and red curve are simulated by discrete-time method with $\Delta t = 0.05$ and $\Delta t = 0.01$, respectively. The yellow one is derived by continuous-time method. The results are averaged over 100 simulations.

**(a)** Relations between metastable prevalence and effective infection rate $\tau$ on continuous-time simulations and discrete-time simulations of adaptive SIS network.



**(b)** Relations between averaged computation time and effective infection rate $\tau$ on continuous-time simulations and discrete-time simulations of adaptive SIS network.

**Figure 4.3:** Continuous-time simulations and discrete-time simulations on adaptive SIS network with size $N = 40$, $\omega = 2$, $\epsilon = 0.001$. Effective infection rate $\tau$ is in range of $(0, 0.3)$, and time period $T = 500$. The blue curve and red curve are simulated by discrete-time method with $\Delta t = 0.05$ and $\Delta t = 0.01$, respectively. The yellow one is derived by continuous-time method. The results are averaged over 100 simulations.

# 5

# Analysis of the time-varying topology

In this chapter, we are going to discuss the impact of the parameters on the metastable-state topology based on a series of numerical simulations using the devised continuous-time simulator.

## 5.1. States of the metastable-state topology

### 5.1.1. The possible states of the epidemic process

Due to the introduction of link dynamics processes, the epidemic dynamics of the adaptive SIS network is altered comparing to the static network. For the static case, we have basically two possible states, i.e., endemic state and disease-free state.Introducing link dynamics, we have an additional behaviour, which is bistability to the steady state, where both endemic state and the disease-free state exist. Therefore, there are in total three states of the adaptive SIS network in the steady state, which are *disease-free state*, *endemic state*, and *bistable state*, which are illustrated in Figure 5.1a, 5.1b and 5.1c, respectively. In the Figure 5.1c, the fraction of infected nodes $y$ is plotted which shows both the endemic state and disease-free state, and hence is called *bistable*.

### 5.1.2. Explanation view: Energy landscape

To map out all possible states of a system, energy landscape is an approach which describes the relation between the states and their corresponding energy level [6, 34]. In our report, we use this method to illustrate the bistability of the metastable topology of an adaptive SIS network. An energy landscape of the adaptive SIS network represents all possible states, including endemic state, disease-free state and bistable state, in the steady state and their potential energy. In our case, the potential energy is as a function of the number of infected nodes in the metastable state in the space. Hills and valleys represent the local maxima and minima in the energy landscape, respectively. The height of the hill depends on the parameters of the adaptive SIS network.

Figure 5.2 shows the energy landscapes for the three different metastable states corresponding various potential energy. When the metastable state is stable in the disease-free state S1 or endemic state S2, it is hard to move the state to climb the hill. Since the energy difference $\Delta E$ is large, the state is stable in the global minimum. When $\Delta E_1$ and $\Delta E_2$ are large in Figure 5.2*c*, where the height of the hill decreases, the state in a valley is possible to reach the unstable equilibrium point (maximum), and potential to move to the other side of valley, as shown in Figure 5.2c.
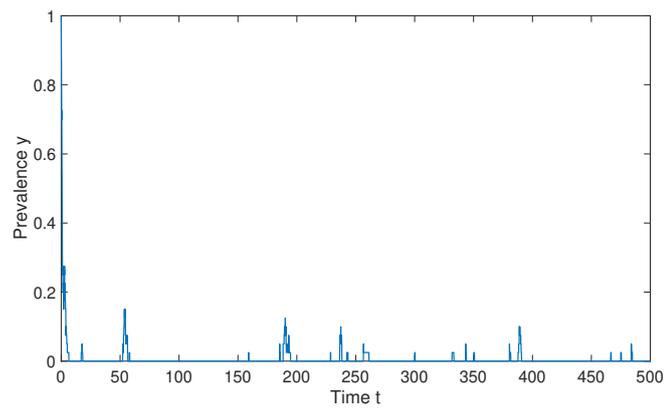
**(a)** *Disease-free state*: A single run of the Markov process of the adaptive SIS network with size $N = 40$, $\tau = 0.05$, $\omega = 1$, $\epsilon = 0.001$.
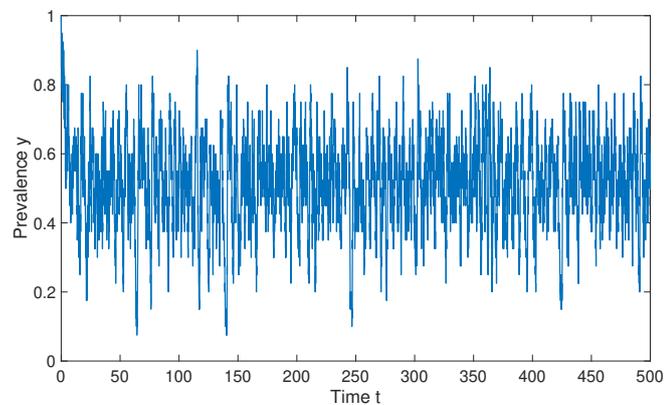


**(b)** *Endemic state*: A single run of the Markov process of the adaptive SIS network with size $N = 40$, $\tau = 0.25$, $\omega = 1$, $\epsilon = 0.001$.
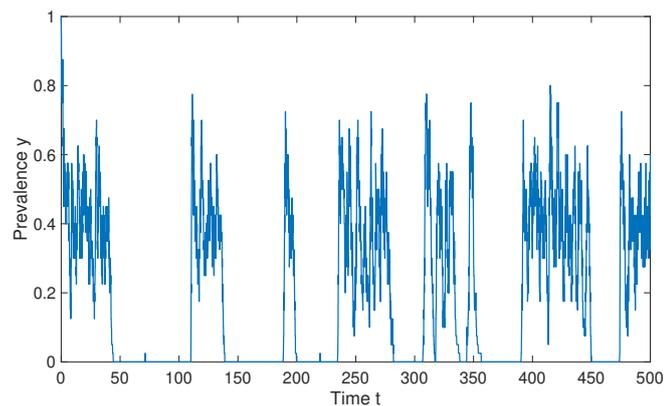


**(c)** *Bistable state*: A single run of the Markov process of the adaptive SIS network with size $N = 40$, $\tau = 0.18$, $\omega = 1$, $\epsilon = 0.001$.

**Figure 5.1:** Markov processes of the adaptive SIS network with size $N = 40$, $\omega = 1$, $\epsilon = 0.001$ and various $\tau$. The simulation period is 50,000 time units. The prevalence in the metastable state might be in three states: (a) disease-free state, (b) endemic state or (c) bistable state.
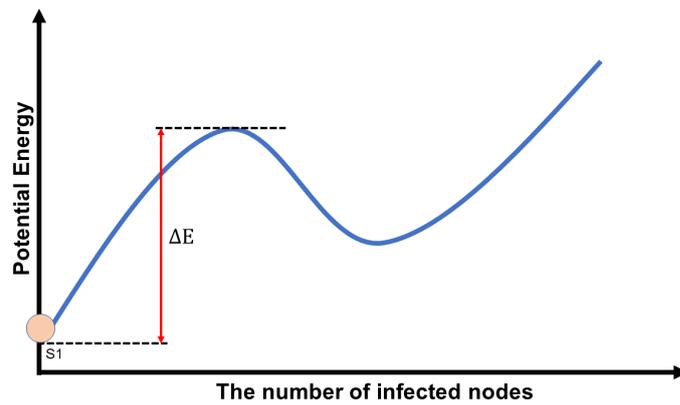
**(a)** System is constrained in the disease-free state due to large energy difference $\Delta E$
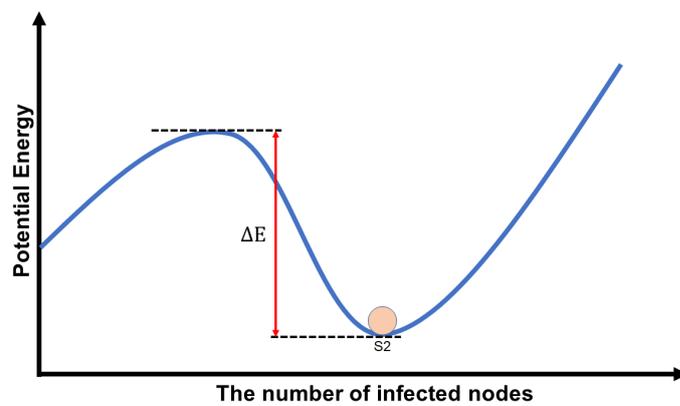


**(b)** System is constrained in the endemic state due to the large energy difference $\Delta E$
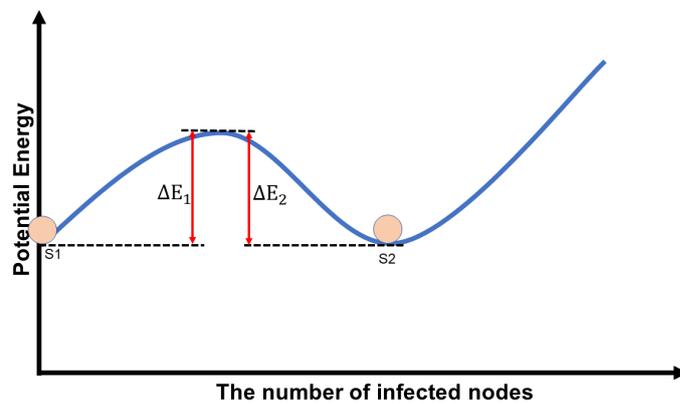


**(c)** System can transfer from the endemic state to the disease-free state or the other way around, leading to the bistable state.

**Figure 5.2:** Energy landscape of possible states in the system. S1: Disease-free state; S2: Endemic state. Hill indicates unstable equilibrium point (maxima) and valleys are the metastable equilibrium points (local minima). $\Delta E$ is the energy difference between the hill and the valley.

### 5.1.3. Classification

In this section, we are going to discuss the relationship between the network parameters, i.e., the effective infection rate $\tau$ and the effective link breaking rate $\omega$, and different types of metastable state. The numerical results allow us to analyze the bistability of the adaptive SIS network, and we would like to show how the SIS process behaves under all circumstances. Therefore, in the simulation, we take a series of $\tau$ and $\omega$ which can affect the endemic equilibrium, and compute the fraction of time period spanned in the disease-free state of the total simulation time. If this fraction is small, it means that during the whole simulation period, most of the time is endemic state, otherwise, it means the disease-free state dominates.

The simulation results are provided in Figure 5.3, which can be regarded as the classification of the aforementioned states. As shown in Figure 5.3, the metastable state stabilizes in the disease-free state on the dark red region for the low $\tau$ which is below the epidemic threshold $\tau_c$ of the adaptive SIS network. For the larger $\omega$, we can observe that the dark red region get wider as $\tau_c$ increases. The endemic state is considered in the dark blue region.

Besides, in the region between orange and light blue, both the disease-free state and endemic state are stable. As either parameter increases, the number of infected nodes in the metastable state increases and the link removal occurs at a high rate. It leads to a lower energy difference $\Delta E$, which mentioned in section 5.1.2, for the bistability. As shown in Figure 5.3, as the value of $\omega$ is high, the region of the bistable state get wider.
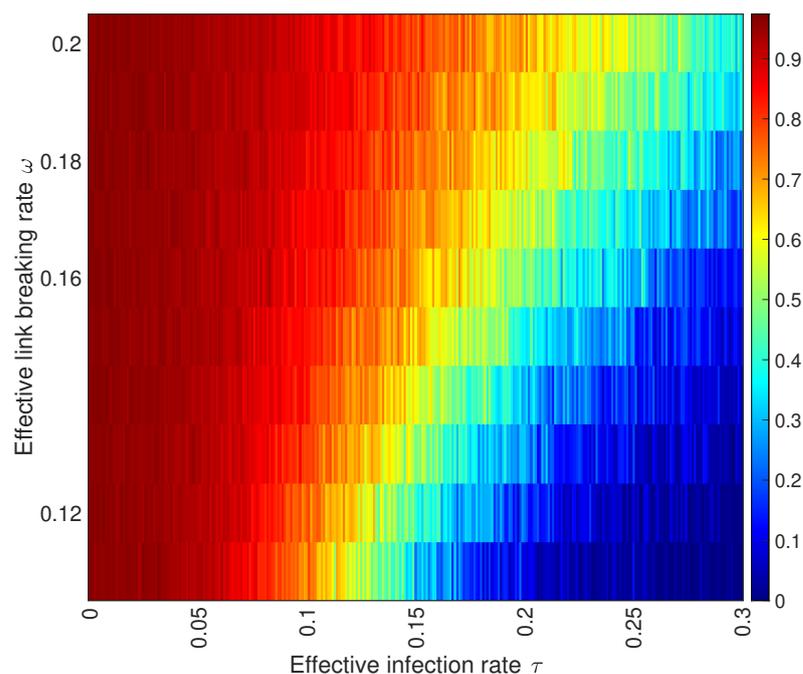


**Figure 5.3:** Fraction of the time period spanned by disease-free state of the total simulating time period for various effective infection rates $\tau$ and effective link-breaking rates $\omega$. We have used $N = 40$, $\zeta = 1$, $\epsilon = 0.001$. A low fraction (red region) means the disease-free state dominates, while a high fraction (blue region) means the endemic state dominates.

## 5.2. Degree distribution

To improve our understanding of the interplay between network topology and dynamics, a good way is to investigate the degree distribution of the adaptive SIS network [25]. Since it

is hard to illustrate the degree distribution over time, we only show some snapshots of the evolution in Figure 5.4. The degree distribution of the initial network is a complete graph with $N = 40$ nodes, and is illustrated as one peaked bar at degree $D = 39$, where all nodes have the same degree $D = N - 1$. In the beginning, all nodes are considered to be infected. When starting evolving, its degree distribution quickly moves to a peaked distribution over time. Obviously, when the number of infected nodes decreases, the distribution shifts to the left and more nodes have lower degrees. As there exist small oscillations in the prevalence, the shape of degree distribution might change slightly in the metastable state. But the metastable-state degree distribution stabilizes to a peak distribution.

When $\tau$ decreases and keeping all other parameters constant, as shown in Figure 5.4a and 5.4b, the meta-stable state degree distribution shifts to right as more nodes in the metastable-state are possibly healthy and more links are reestablished, increasing the average degree. When $\omega$ is large, the endemic steady state acts like the bistable state, including endemic state and disease-free state. Then the metastable degree distribution in Figure 5.4d is not a centralized peaked distribution but a peaked distribution with another peaked bar at $D = 39$.

### 5.2.1. Classification of binomial-like distribution and non-binomial distribution

We observe that the degree distribution of adaptive SIS network in the metastable state is seemingly similar to a binomial distribution under some circumstances, see for example Figure 5.4a yellow histogram. Therefore, it would be interesting to investigate whether the shape of the degree distribution is binomial-like. In order to do so, we first need to generate a binomial distribution. The binomial distribution $B(n, p)$ of the degree $D$ is formulated as follows

$$\Pr[D = k] = \binom{n}{k} \cdot p^k (1-p)^{n-k}, \tag{5.1}$$

where $n$ denotes the number of independent experiments and $p$ is the success probability. In our case, $n$ has the value of the largest degree and $p$ is the probability of establishing a link.

For variable following the binomial distribution, the mean value $m$ can be derived by $np$. Using the degree distribution of the adaptive SIS network, we can estimate a binomial distribution $B(n, p)$, where $n$ and $m$ are maximum value and average value of the metastable degrees, respectively. Then the $p$ parameter of the binomial distribution can be estimated as

$$p = \frac{m}{n}.$$

To compare the difference between the degree distribution and the estimated binomial distribution, here we use the Euclidean distance to describe the difference between two distributions. First, we represent each of the distribution using a vector $\mathbf{d}$, where the entry is filled with the corresponding probability density, i.e., $[\mathbf{d}]_i = \Pr[D = i]$. Second, we can compute the $l_2$−norm of the difference between two vectors, i.e.,

$$\mathcal{E} = \|\mathbf{d}_s - \mathbf{d}_e\|_2, \tag{5.2}$$

where $\mathcal{E}$ is error, subscripts $s$ and $e$ represent *simulation* and *estimation*, respectively.

For example, in Figure 5.5a, the binomial distribution (red curve) could fit the degree distribution well as the distance error in between is 0.016, which is small. Thus this degree distribution seems to follow a binomial distribution. However, Figure 5.5b shows that the degree distribution is not a binomial distribution due to a large error 0.36.
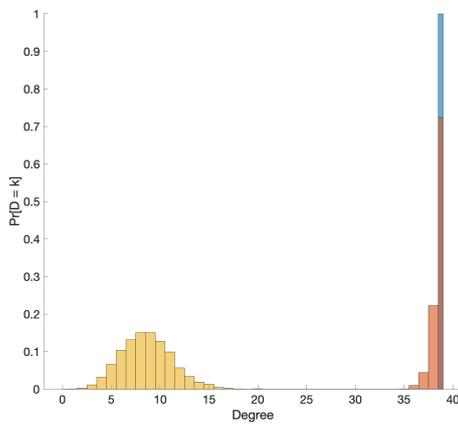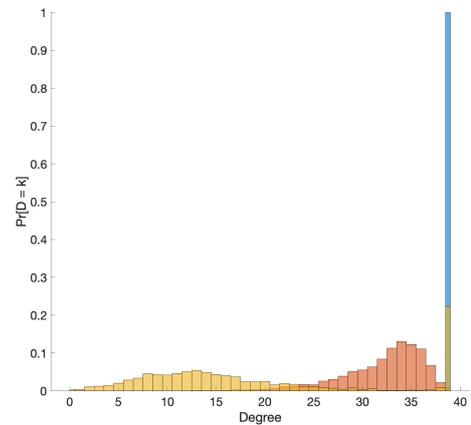
**(a)** Snapshot of degree distribution of adaptive SIS network with $N = 40$, $\tau = 0.5$, $\omega = 1$, $\zeta = 0.1$, $\epsilon = 0.001$.
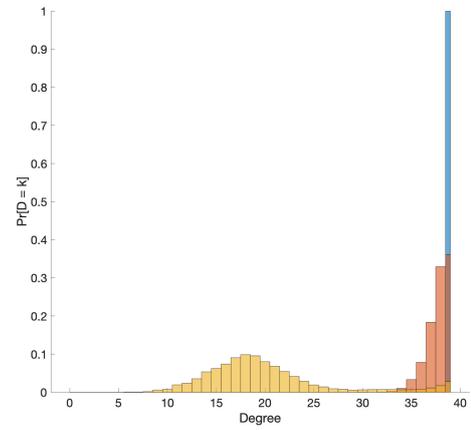


**(b)** Snapshot of degree distribution of adaptive SIS network with $N = 40$, $\tau = 0.1$, $\omega = 1$, $\zeta = 0.1$, $\epsilon = 0.001$.
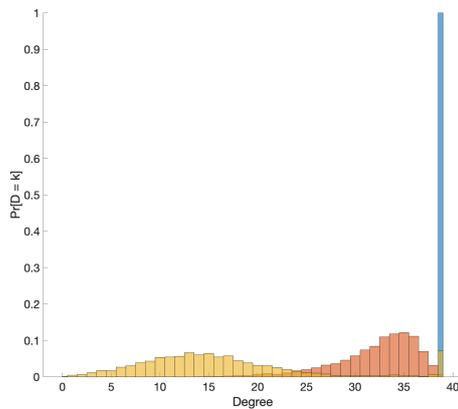


**(c)** Snapshot of degree distribution of adaptive SIS network with $N = 40$, $\tau = 0.2$, $\omega = \zeta = 1$, $\epsilon = 0.001$.



**(d)** Snapshot of degree distribution of adaptive SIS network with $N = 40$, $\tau = 0.5$, $\omega = 2$, $\zeta = 1$, $\epsilon = 0.001$.

**Figure 5.4:** Snapshots of the degree distribution for adaptive SIS network with size $N = 40$. The blue bar is the initial degree distribution at $t = 0$, the orange histogram shows the network for small times, and the yellow histogram shows the degree distribution in the metastable state.
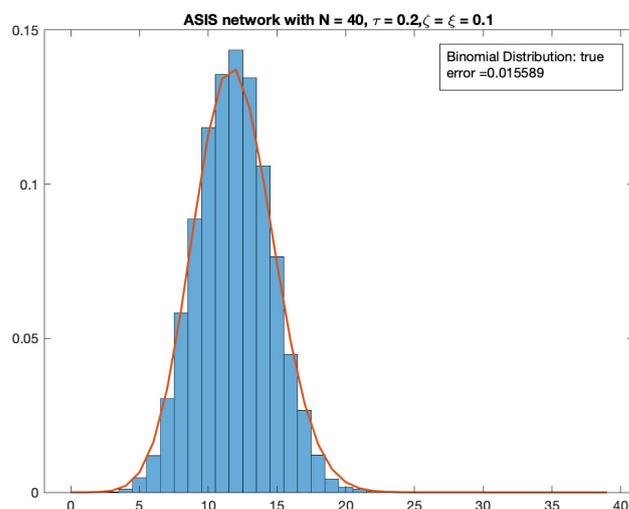
**(a)** Comparison between a binomial distribution and the metastable-state degree distribution for adaptive SIS network with parameters $N = 40$, $\tau = 0.2$, $\omega = 1$, $\zeta = 0.1$, $\epsilon = 0.001$.
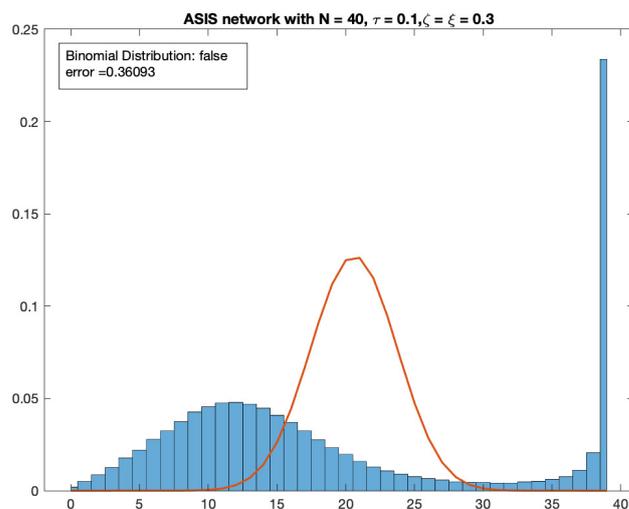


**(b)** Comparison between a binomial distribution and the metastable-state degree distribution for adaptive SIS network with parameters $N = 40$, $\tau = 0.1$, $\omega = 1$, $\zeta = 0.3$, $\epsilon = 0.001$.

**Figure 5.5:** Comparison between a binomial distribution and the metastable-state degree distribution for adaptive SIS network. The red curve is a binomial distribution and the blue bar is the metastable-state degree distribution.
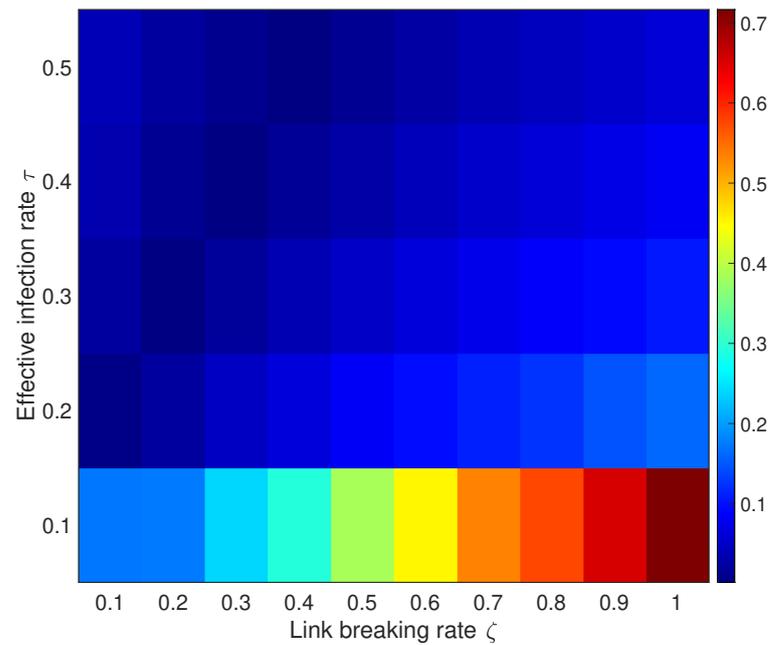
**Figure 5.6:** Binomial fitting error of the degree distribution. The fitting error is plotted as a function of the effective infection rate $\tau$ and link breaking rate $\zeta$ from continuous-time simulations of the adaptive SIS network with $N = 40$, $\omega = 1$, and various $\tau$ and $\zeta$.

We would like to see whether the degree distribution follows the binomial distribution for any value of the parameters $\tau$ and $\zeta$. In order to quantify the relation between the parameters and degree distribution, we compute the binomial fitting error of the degree distribution using Equation (5.2) and then plot the error as a function of the effective infection rate $\tau$ and link breaking rate $\zeta$, in Figure 5.6. As $\tau$ decreases and $\zeta$ increases, the disease prevalence $y$ decreases. As a result the degree distribution becomes flatter. Thus we can observe that the distance error between the degree distribution and the binomial distribution increases with higher effective infection rate $\tau$. Moreover, in Figure 5.6, the degree distribution is classified as the binomial-like distribution in the dark blue part for the low fitting error which is below 0.2.

<div style="text-align: right">

# 6

</div>

# Conclusion and Future work

## 6.1. Conclusion

This thesis work can be divided into two parts. In the first part, we developed the continuous-time simulator for the adaptive SIS network. This is because the spreading process over the adaptive network is a continuous stochastic process and in the previous works, only the discrete-time simulator serving as an approximation was implemented. In this part, we first introduced the Gillespie algorithm, the core of the continuous-time simulator. Based on this algorithm, we developed the new simulator. Furthermore, using the devised simulator, we illustrated the accuracy of the discrete-time simulations compared to the real continuous-time simulations. From our numerical simulation results, we can demonstrate that if the discrete time step $\Delta t$ becomes infinitesimal, then there would be no difference between the two simulators. But with various parameters of ASIS network, the discrete-time simulator requires different time step to simulate accurately. Regarding the computation time, since the Gillespie algorithm is an event-driven algorithm, the continuous-time simulator requires less time for small value of parameters. But when the parameters becomes larger, then the required time increases.

In the second part, we performed various of simulations using the proposed simulator, and based on these simulations, we discussed the impact of the parameters, e.g., effective infection rate $\tau$, effective link breaking rate $\omega$, and link breaking rate $\zeta$, on the state of the network and the degree distribution of the network. Under this circumstance, there exist three states in the network, which are disease-free state, endemic state and bistable state. In the numerical results, we illustrated that when $\omega$ is large and $\tau$ is small, the system tends to be disease-free state, and when $\omega$ is small and $\tau$ is large, the system tends to be in the endemic state. As either parameter increases, the number of infected nodes in the metastable state increases and the link removal occurs at a high rate. Changes of these parameters can destabilize the metastable state so that the system tends to be in the bistable state.

We also investigated the degree distribution in the metastable state. We observed that in some cases, it followed the binomial distribution while in other cases it did not. In order to investigate the relationship between parameters and distribution behaviour, we measured the difference between the degree distribution and the binomial distribution. Our results show that when $\tau$ is large and $\zeta$ is small, the distribution tends to be binomial-like, and when $\tau$ is small and $\zeta$ is large, the distribution does not follow the binomial distribution.

## 6.2. Future work

- In this thesis, we initialise the simulations using the complete graph. However, it is interesting but still unknown how the system would behave when taking other network models, such as Erdős-Rényi graph model, scale-free graph model or small world graph model, as the initial condition.

- This thesis work is mostly based on the numerical method. Although the simulation results have already shown some properties of the adaptive SIS network, it would be interesting if this problem is viewed from the perspective of the theoretical analysis.

- In the continuous simulator, we only consider the adaptive SIS process over the network. However, there exist various of models regarding the link dynamic process other than the adaptive SIS process, e.g., adaptive information diffusion (AID) model [17, 28]. It would be interesting to investigate the continuous simulator for these models.

# A

## Appendix
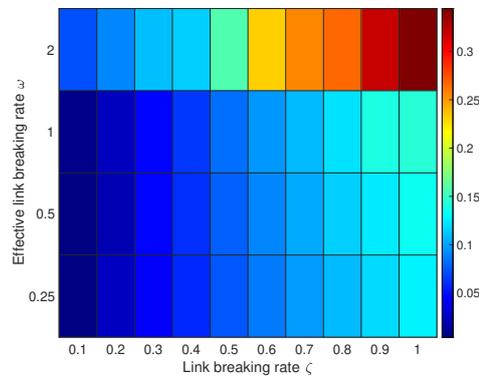


**Figure A.1:** Binomial fitting error of the degree distribution with various effective link breaking rate $\omega$ and link breaking rate $\zeta$. Simulations are on the adaptive SIS network with $N = 40$, $\tau = 0.2$, and various $\omega$ and $\zeta$.
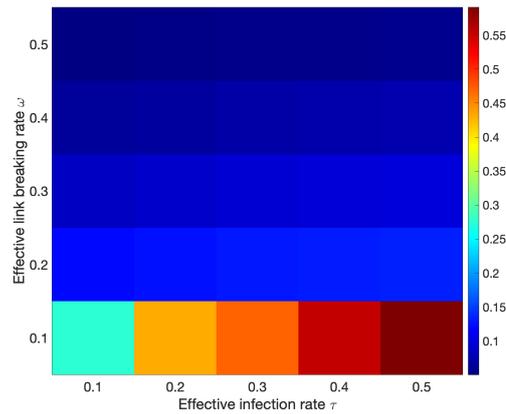


**Figure A.2:** Binomial fitting error of the degree distribution with various effective infection rate $\tau$ and effective link breaking rate $\omega$. Simulations are on the adaptive SIS network with $N = 40$, $\zeta = 1$, and various $\omega$ and $\tau$.
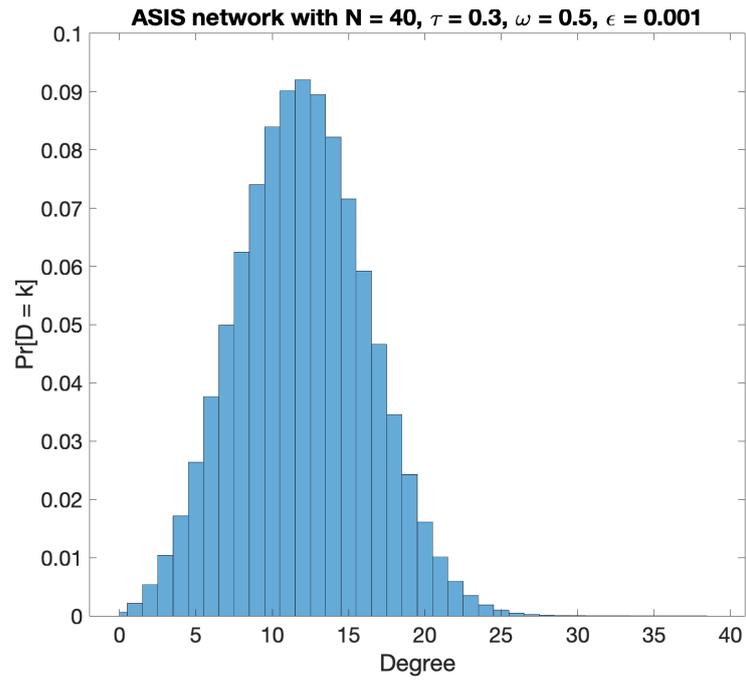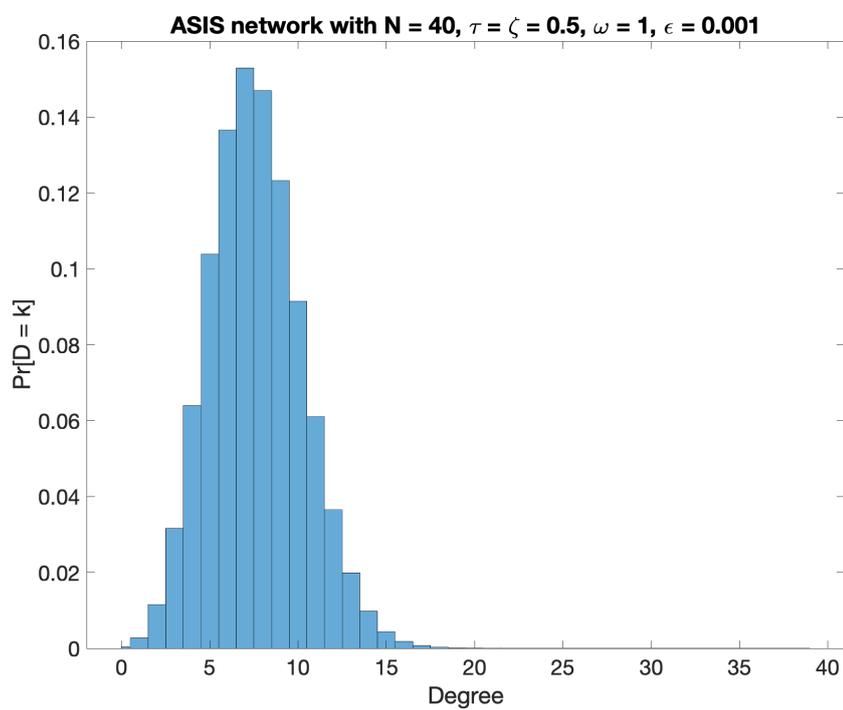
**Figure A.3:** Degree distribution of the adaptive SIS network with $N = 40$, $\tau = 0.3$, $\omega = 0.5$, $\zeta = 1$, and $\epsilon = 0.001$.
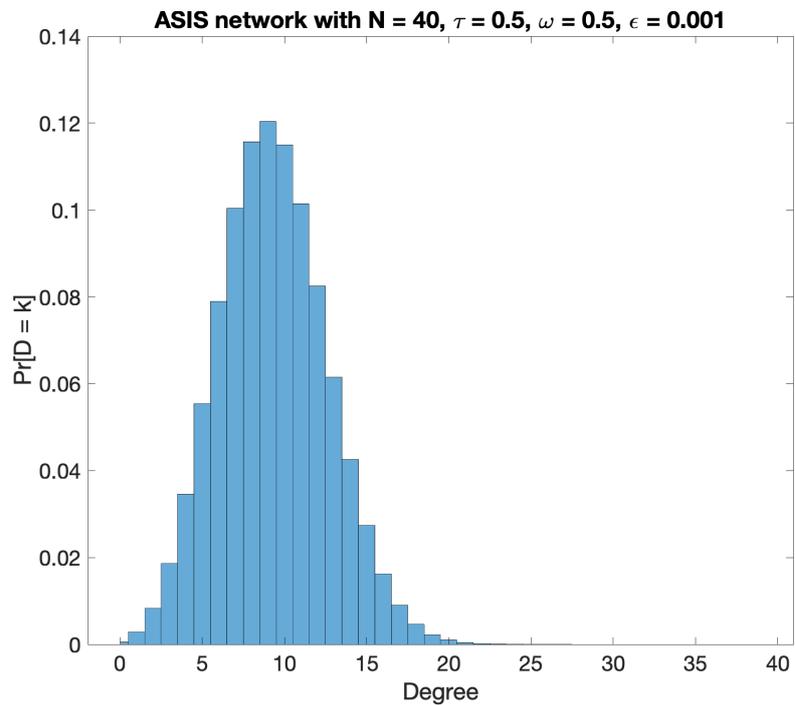


**Figure A.4:** Degree distribution of the adaptive SIS network with $N = 40$, $\tau = 0.5$, $\omega = 0.5$, $\zeta = 1$, and $\epsilon = 0.001$.
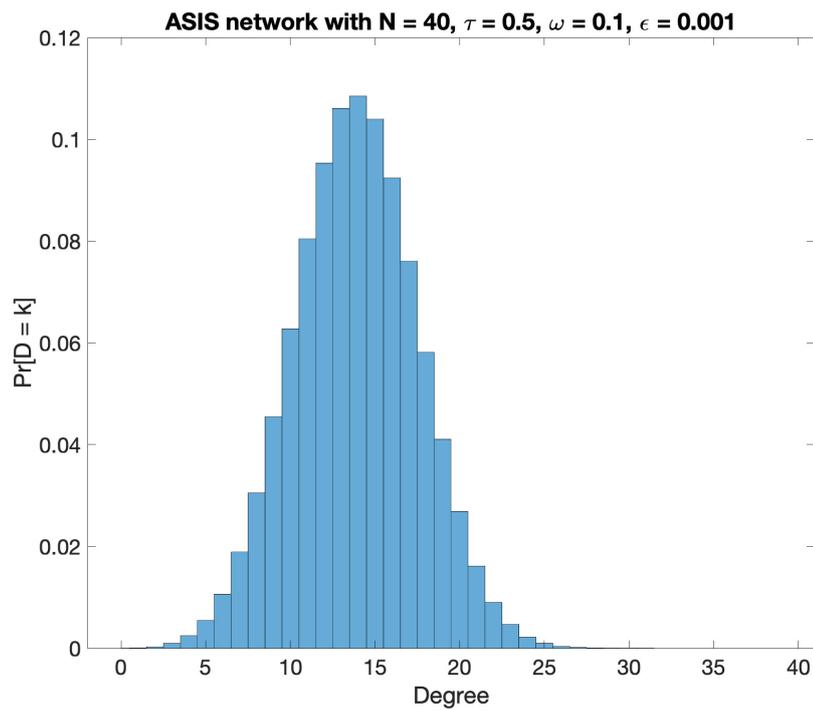
**Figure A.5:** Degree distribution of the adaptive SIS network with $N = 40$, $\tau = 0.5$, $\omega = 0.1$, $\zeta = 1$, and $\epsilon = 0.001$.
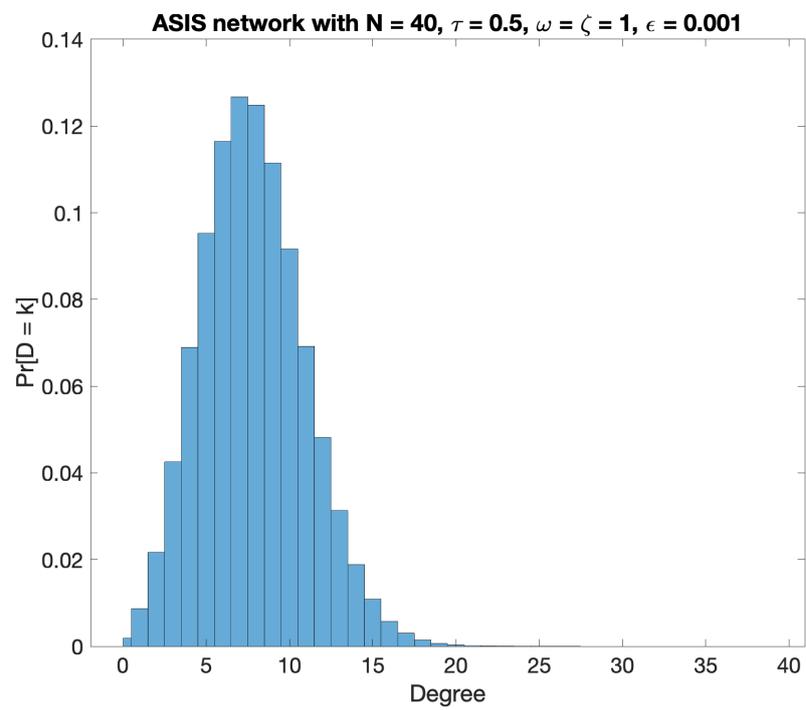


**Figure A.6:** Degree distribution of the adaptive SIS network with $N = 40$, $\tau = \zeta = 0.5$, $\omega = 1$, and $\epsilon = 0.001$.
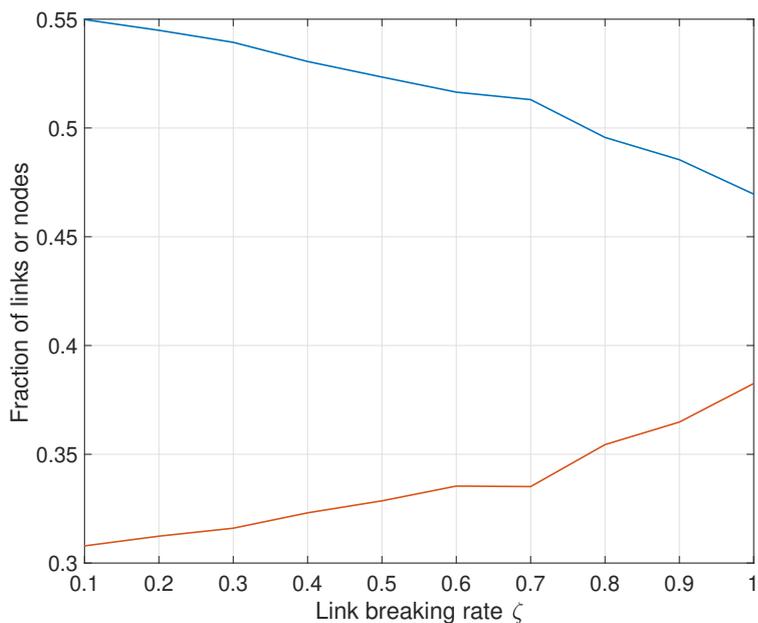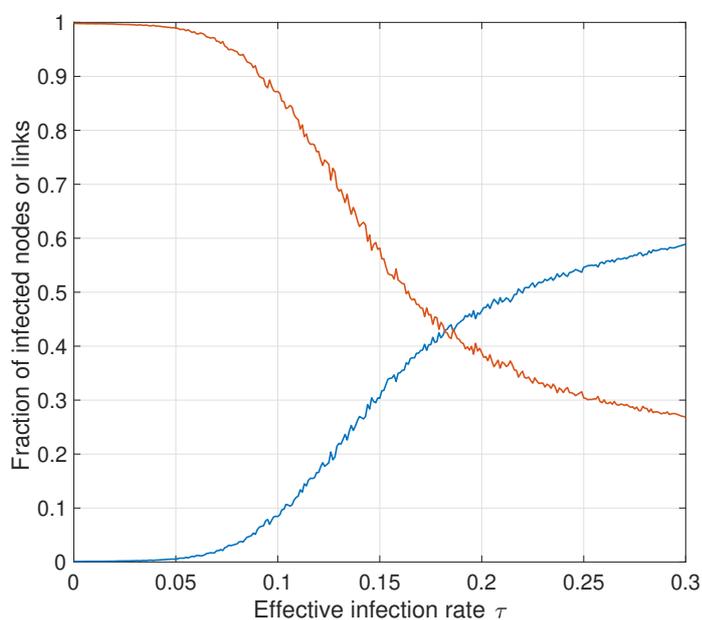
**Figure A.7:** Degree distribution of the adaptive SIS network with $N = 40$, $\tau = 0.5$, $\omega = \zeta = 1$, and $\epsilon = 0.001$.

**Figure A.8:** Relations between metastable prevalence and link breaking rate $\zeta$ of the adaptive SIS network with $N = 40$, $\tau = 0.2$, $\omega = 1$. The blue curve is the fraction of infected nodes with various $\zeta$ and the red curve is the fraction of links with various $\zeta$.



**Figure A.9:** Relations between metastable prevalence and effective infection rate $\tau$ of the adaptive SIS network with $N = 40$, $\omega = \zeta = 1$. The blue curve is the fraction of infected nodes with various $\tau$ and the red curve is the fraction of links with various $\tau$.

# Bibliography

[1] What is prevalence? https://www.nimh.nih.gov/health/statistics/what-is-prevalence.shtml.

[2] Massimo Achterberg. Modelling markovian epidemic and information diffusion over adaptive networks. 2019.

[3] Massimo A Achterberg, Johan LA Dubbeldam, Cornelis J Stam, and Piet Van Mieghem. Classification of link-breaking and link-creation updating rules in susceptible-infected-susceptible epidemics on adaptive networks. *Physical Review E*, 101(5): 052302, 2020.

[4] Massimo A Achterberg, Bastian Prasse, Long Ma, Stojan Trajanovski, Maksim Kitsak, and Piet Van Mieghem. Comparing the accuracy of several network-based covid-19 prediction algorithms. *International journal of forecasting*, 2020.

[5] Linda JS Allen. Some discrete-time si, sir, and sis epidemic models. *Mathematical biosciences*, 124(1):83–105, 1994.

[6] Andrew J Ballard, Ritankar Das, Stefano Martiniani, Dhagash Mehta, Levent Sagun, Jacob D Stevenson, and David J Wales. Energy landscapes for machine learning. *Physical Chemistry Chemical Physics*, 19(20):12585–12603, 2017.

[7] Frederick H Chen. A susceptible-infected epidemic model with voluntary vaccinations. *Journal of mathematical biology*, 53(2):253–272, 2006.

[8] Domenico Cucinotta and Maurizio Vanelli. Who declares covid-19 a pandemic. *Acta Bio Medica: Atenei Parmensis*, 91(1):157, 2020.

[9] Daniel T Gillespie. A general method for numerically simulating the stochastic time evolution of coupled chemical reactions. *Journal of computational physics*, 22(4):403–434, 1976.

[10] Daniel T Gillespie. Exact stochastic simulation of coupled chemical reactions. *The journal of physical chemistry*, 81(25):2340–2361, 1977.

[11] Thilo Gross, Carlos J Dommar D'Lima, and Bernd Blasius. Epidemic dynamics on an adaptive network. *Physical review letters*, 96(20):208701, 2006.

[12] Dongchao Guo, Stojan Trajanovski, Ruud van de Bovenkamp, Huijuan Wang, and Piet Van Mieghem. Epidemic threshold and topological structure of susceptible-infectious-susceptible epidemics in adaptive networks. *Physical Review E*, 88(4): 042802, 2013.

[13] Brian Karrer and Mark EJ Newman. Message passing approach for general epidemic models. *Physical Review E*, 82(1):016101, 2010.

[14] Matt J Keeling and Ken TD Eames. Networks and epidemic models. *Journal of the royal society interface*, 2(4):295–307, 2005.

[15] William Ogilvy Kermack and Anderson G McKendrick. Contributions to the mathematical theory of epidemics. ii.—the problem of endemicity. *Proceedings of the Royal Society of London. Series A, containing papers of a mathematical and physical character*, 138(834):55–83, 1932.

[16] Cecilia Lagorio, Mark Dickison, Federico Vazquez, Lidia A Braunstein, Pablo A Macri, MV Migueles, Shlomo Havlin, and H Eugene Stanley. Quarantine-generated phase transition in epidemic spreading. *Physical Review E*, 83(2):026102, 2011.

[17] Yunhan Long. *Spread and interaction of epidemics and information on adaptive social networks*. The College of William and Mary, 2015.

[18] Naoki Masuda and Luis EC Rocha. A gillespie algorithm for non-markovian stochastic processes. *Siam Review*, 60(1):95–115, 2018.

[19] Joel C Miller and Tony Ting. Eon (epidemics on networks): a fast, flexible python package for simulation, analytic approximation, and analysis of epidemics on networks. *arXiv preprint arXiv:2001.02436*, 2020.

[20] Masaki Ogura and Victor M Preciado. Epidemic processes over adaptive state-dependent networks. *Physical Review E*, 93(6):062316, 2016.

[21] Romualdo Pastor-Satorras, Claudio Castellano, Piet Van Mieghem, and Alessandro Vespignani. Epidemic processes in complex networks. *Reviews of modern physics*, 87(3):925, 2015.

[22] Bastian Prasse, Massimo A Achterberg, Long Ma, and Piet Van Mieghem. Network-inference-based prediction of the covid-19 epidemic outbreak in the chinese province hubei. *Applied Network Science*, 5(1):1–11, 2020.

[23] Matheus Henrique Dal Molin Ribeiro, Ramon Gomes da Silva, Viviana Cocco Mariani, and Leandro dos Santos Coelho. Short-term forecasting covid-19 cumulative confirmed cases: Perspectives for brazil. *Chaos, Solitons & Fractals*, 135:109853, 2020.

[24] Masaki Sekiguchi and Emiko Ishiwata. Global dynamics of a discretized sirs epidemic model with time delay. *Journal of Mathematical Analysis and Applications*, 371(1): 195–202, 2010.

[25] N Sherborne, KB Blyuss, and IZ Kiss. Bursting endemic bubbles in an adaptive network. *Physical Review E*, 97(4):042306, 2018.

[26] Ye Sun, Long Ma, An Zeng, and Wen-Xu Wang. Spreading to localized targets in complex networks. *Scientific reports*, 6(1):1–10, 2016.

[27] Biao Tang, Fan Xia, Sanyi Tang, Nicola Luigi Bragazzi, Qian Li, Xiaodan Sun, Juhua Liang, Yanni Xiao, and Jianhong Wu. The effectiveness of quarantine and isolation determine the trend of the covid-19 epidemics in the final phase of the current outbreak in china. *International Journal of Infectious Diseases*, 95:288–293, 2020.

[28] Stojan Trajanovski, Dongchao Guo, and Piet Van Mieghem. From epidemics to information propagation: Striking differences in structurally similar adaptive network models. *Physical Review E*, 92(3):030801, 2015.

[29] Ilker Tunc, Maxim S Shkarayev, and Leah B Shaw. Epidemics in adaptive social networks with temporary link deactivation. *Journal of statistical physics*, 151(1):355–366, 2013.

[30] Piet Van Mieghem. *Performance analysis of complex networks and systems*. Cambridge University Press, 2014.

[31] Piet Van Mieghem and Eric Cator. Epidemics in networks with nodal self-infection and the epidemic threshold. *Physical Review E*, 86(1):016116, 2012.

[32] Piet Van Mieghem, Jasmina Omic, and Robert Kooij. Virus spread in networks. *IEEE/ACM Transactions On Networking*, 17(1):1–14, 2008.

[33] Christian L Vestergaard and Mathieu Génois. Temporal gillespie algorithm: Fast simulation of contagion processes on time-varying networks. *PLoS computational biology*, 11(10):e1004579, 2015.

[34] David J Wales. Exploring energy landscapes. *Annual review of physical chemistry*, 69: 401–425, 2018.

[35] Jie Zhou, Gaoxi Xiao, Siew Ann Cheong, Xiuju Fu, L Wong, Stefan Ma, and Tee Hiang Cheng. Epidemic reemergence in adaptive complex networks. *Physical Review E*, 85 (3):036107, 2012.